isvr Institute of Sound and Vibration Research

Finite Element Analysis of the Vibrations of Waveguides and Periodic Structures

D. Duhamel, B.R. Mace and M.J. Brennan

ISVR Technical Memorandum 922

August 2003

University of Southampton

SCIENTIFIC PUBLICATIONS BY THE ISVR

Technical Reports are published to promote timely dissemination of research results by ISVR personnel. This medium permits more detailed presentation than is usually acceptable for scientific journals. Responsibility for both the content and any opinions expressed rests entirely with the author(s).

Technical Memoranda are produced to enable the early or preliminary release of information by ISVR personnel where such release is deemed to the appropriate. Information contained in these memoranda may be incomplete, or form part of a continuing programme; this should be borne in mind when using or quoting from these documents.

Contract Reports are produced to record the results of scientific work carried out for sponsors, under contract. The ISVR treats these reports as confidential to sponsors and does not make them available for general circulation. Individual sponsors may, however, authorize subsequent release of the material.

UNIVERSITY OF SOUTHAMPTON

INSTITUTE OF SOUND AND VIBRATION RESEARCH

DYNAMICS GROUP

Finite Element Analysis of the Vibrations of Waveguides and Periodic Structures

by

D. Duhamel, B.R. Mace and M.J. Brennan

ISVR Technical Memorandum No: 922

August 2003

Authorised for issue by
Professor M.J. Brennan
Group Chairman

Abstract

Many structures present symmetry in one direction, which can be a periodicity in the case of several identical cells or translation or rotation symmetry in case of a waveguide. The purpose of this work is first to present a common analysis of these two types of structures. Then from the dynamic stiffness matrix of a cell of the structure obtained by a standard finite element package, we present an efficient method for calculating the response of the complete structures to harmonic excitations. Thus a very general structure can be meshed with standard FE software and the calculations are not limited to simple analytical examples. The method consists in using a wave basis to describe the vibrations of the structure instead of the traditional modal shapes. This wave basis is obtained from the eigenvectors of the transfer matrix of the periodic cell. Then the classical dynamic stiffness matrix can be built from these wave modes. The computational cost becomes independent of the number of cells in the structures, which is a major improvement over the classical finite element analysis for large structures. The main advantage of the approach over alternative waveguide/FE approaches, often termed spectral elements, is that conventional FE packages can be used to form the stiffness and mass matrices.

Contents

1. Introduction

We often have to deal with structures presenting symmetry in one direction. This symmetry, as shown in figure 1, can be a translation according to a privileged direction (a), a rotational symmetry (b) or a periodicity (c). To solve a dynamic problem with such structures, for instance the calculation of the frequency response function between an excitation force and a reception point, classical finite element software often offers no other choice than meshing the whole structure. Exceptions are rotational and cyclic symmetries, which are solved by a decomposition of the displacements in cosine and sine functions. A review of the current practises for these structures can be found in Wang [1]. However, a better use of the symmetry could lead to a much more efficient computation.

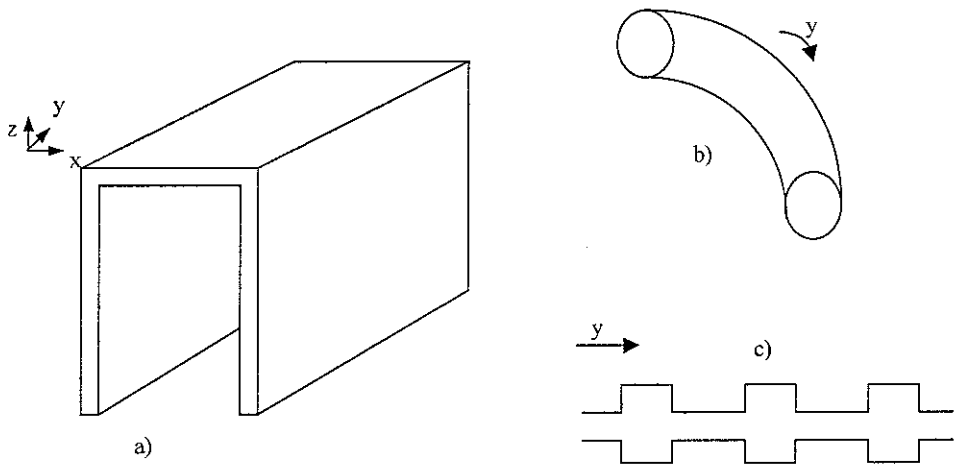

Figure 1: Different structures with symmetries along the *y* direction

Many previous works have considered such structures. They can be classified into the classical analysis of periodic structures and more recently the analysis of structures with constant cross-section by the waveguide finite elements, often called the spectral finite element approach. The purpose of this paper is first to make a link between these two approaches, then to show how the dynamic, finite element analysis of periodic structures can be improved and finally present a method to get a waveguide finite element model for general structures from standard finite element software. If we compare to standard FE approaches, the cost of a calculation with the model developed in this paper is greatly reduced because we only have to mesh one cell instead of the whole structure. We get, although, a frequency domain model but with a well-posed formulation, without numerical problem. The other advantage is that standard FE packages can be used on the contrary of spectral FE, which need to develop new elements for each application.

1.1 Periodic structures

The propagation of waves in periodic structures is an old subject; see for instance the work of Brillouin [2] and the review paper of Mead [3] presenting the research from Southampton in this field. The approach is based on the Floquet's principle or the transfer matrix. The basic idea is that the propagation of waves in a periodic structure can be obtained from propagation constants λ, which depend on the frequency, or by the transfer matrix $\mathbf{T}$, which relates the displacements $\mathbf{q}$ and the forces $\mathbf{f}$ on both sides of the periodic element by the relation (L: left side, R: right side)

$$\begin{bmatrix} \mathbf{q}_R \\ -\mathbf{f}_R \end{bmatrix} = \mathbf{T} \begin{bmatrix} \mathbf{q}_L \\ \mathbf{f}_L \end{bmatrix} = \lambda \begin{bmatrix} \mathbf{q}_L \\ \mathbf{f}_L \end{bmatrix} \tag{1.1}$$

Mead presented a general theory for wave propagation in such periodic systems in [4-6]. It was shown that the number of wave is twice the minimum number of degrees of freedom at coupling interfaces and can be decomposed in an equal number of positive and negative-going waves. The propagation constants λ are the eigenvalues of a transfer matrix $\mathbf{T}$ and can be written as $\lambda = e^{ikl}$ where l is the length of the periodic cell and k a wavenumber.

The purpose of most articles is to calculate the dispersion relations. These relations describe the dependence of the wavenumbers k on frequency. They show bands with real wavenumbers corresponding to propagating waves and bands with complex wavenumbers leading to attenuating waves. Mead [4-6] also derived relations between the upper and lower frequency limits of propagation bands and natural frequencies of a single element. These works are mainly of a theoretical nature and the applications deal with simple structures like beams or shells with stiffeners and are solved by analytical means, see for instance Mead [7].

To numerically calculate the dispersion curves, a simple approach consists of prescribing the propagation constant and looking for the frequencies by solving a classical eigenvalue problem with modified stiffness matrices. Orris and Petyt [8] proposed to calculate the propagation constants by the finite element method. They applied their method to beams and skin-rib structures to calculate the eigenfrequencies according to the propagation constants and they plotted the variation of propagation constants with frequency. The use of the finite element method was also explored on more general problems by Abdel-Rahman [9]. A less obvious approach is to set the frequency of interest and to look for the complex propagation constants associated with this frequency by solving the eigenvalue problem of the transfer matrix. Abdel-Rahman [9] also gave examples of application of this reverse problem. For instance, Thompson [10] used this theory of periodic structures for calculating rail vibrations for high frequencies.

1.2 *Waveguide structures*

Structures with constant cross-sections and rotational or a translation symmetry like (a) or (b) in figure 1 are better seen as waveguides. For instance, von Flotow [11] and Beale [12] used this wave approach to study the disturbance propagation in structural networks composed of beam elements and solved the problem by analytical methods. They stated the propagation in each element and the relations at the junction between elements or at boundary conditions. The efficiency is greatly improved compared to FEM methods as a complete beam can be modelled with only one element for any frequency.

For more general structures, the displacements in the cross-section can be described by a finite element method while the variation along the symmetry axis is expressed as an ordinary differential equation whose solution can be written in the form $e^{iky}\mathbf{U}(x,z)$ if y is the direction of symmetry and x and z the coordinates in the cross-section. For instance, Finnveden [13] developed the waveguide approach for different structures and showed that the discrete FEM equation can be put in the form,

$$\left[\sum_{i=1}^{i=N}(k)^i\mathbf{K}_i-\omega^2\mathbf{M}\right]\mathbf{U}=0 \tag{1.2}$$

where $\mathbf{M}$ is the usual mass matrix. The stiffness matrix is developed for various powers of the wavenumber k, describing the propagation in the direction of symmetry, and different $\mathbf{K}_i$ matrices. These are not standard matrices of the finite element formulation and so they must be determined for each problem by methods like Lagranges's equations, Hamilton's principle or the virtual work principle. So for each type of element a complete analysis is needed, which starts by the development of special elements allowing the calculation of the matrices $\mathbf{K}_i$. This makes the connection with the standard use of the finite element method difficult and does not allow the benefits of powerful existing finite element software to be exploited.

For instance, Nilsson [14] used the waveguide finite element to study structures made of plates and shells. Shorter [15] developed waveguide finite elements for viscoelastic laminates and set the discrete problem using Lagrange's equations. He solved for the wavenumber at a given frequency and hence found dispersion relations. Gry [16] applied similar ideas to the calculation of wave propagation in rails with a finite element mesh of a rail cross-section. He then calculated dispersion relations and accelerances. This work was further extended in [17] to take into account the periodic structure of the track by solving the problem in term of a transfer matrix approach.

1.3 *Present paper*

In this paper we present a method, based on the study of periodic structures, to calculate structures like those of figure 1 using models coming from general FEM package like Ansys. From the dynamic stiffness matrix of a cell of the structure obtained by Ansys, we present an efficient method for calculating the wavenumbers of free wave propagation and the response of the complete structure to harmonic

excitations. The objective is to use a wave basis to describe the structure instead of a traditional modal basis. This approach is quite familiar to that used in analytical models. However, we show how to solve some problems specific to the finite element method and conditioning problems. So structures with very general cross-sections can be meshed with standard FEM software.

With the usual finite element methods, as is well known, an increase in the frequency of analysis needs a decrease in the mesh size and a common criterion for a good mesh is to have between 5 and 10 nodes per wavelength. Of course this requirement can lead to large meshes and very heavy calculations for medium and high frequencies. On the contrary, in the proposed method the calculation time is independent of the number of cells in the structures. This allows using a much larger number of cells and leads to efficient high frequencies computations.

The paper is divided into three parts. First we present the finite element analysis of periodic structures. Then we set the general methodology for the analysis of wave propagation in periodic structures. Finally, this is applied to several examples like rods, beams and plates.

2. Finite element analysis of periodic structures

2.1 Cell dynamics

We consider the structure presented in Figure 2. This structure is made of a finite or an infinite number of cells numbered by n. The cells are meshed with an equal number of nodes on their left and right sides.

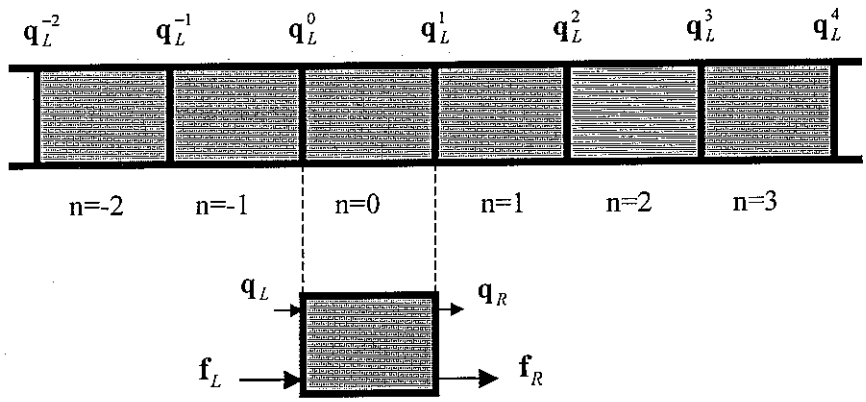

Figure 2: Forces and displacements on a cell.

The discrete dynamic equation of a cell obtained from the finite element model at a frequency ω is given by

$$\left(\mathbf{K} - i\omega\mathbf{C} - \omega^2\mathbf{M}\right)\mathbf{q} = \mathbf{F} \tag{2.1}$$

Where **K**, **M**, and **C** are respectively the stiffness, mass and damping matrices, **F** is the loading vector and **q** the vector of the displacement degrees of freedom. Introducing the dynamic stiffness matrix $\widetilde{\mathbf{D}} = \mathbf{K} - i\omega\mathbf{C} - \omega^2\mathbf{M}$ and decomposing into right (R) and left (L) boundaries and interior (I) degrees of freedom, one gets the following partition of the matrix, in the case where there is no external force on the interior nodes,

$$\begin{bmatrix} \widetilde{\mathbf{D}}_{II} & \widetilde{\mathbf{D}}_{IL} & \widetilde{\mathbf{D}}_{IR} \\ \widetilde{\mathbf{D}}_{LI} & \widetilde{\mathbf{D}}_{LL} & \widetilde{\mathbf{D}}_{LR} \\ \widetilde{\mathbf{D}}_{RI} & \widetilde{\mathbf{D}}_{RL} & \widetilde{\mathbf{D}}_{RR} \end{bmatrix} \begin{bmatrix} \mathbf{q}_I \\ \mathbf{q}_L \\ \mathbf{q}_R \end{bmatrix} = \begin{bmatrix} \mathbf{0} \\ \mathbf{f}_L \\ \mathbf{f}_R \end{bmatrix} \tag{2.2}$$

The interior degrees of freedom can be eliminated using the first relation in (2.2) and this gives

$$\mathbf{q}_I = -\widetilde{\mathbf{D}}_{II}^{-1}\left(\widetilde{\mathbf{D}}_{IL}\mathbf{q}_L + \widetilde{\mathbf{D}}_{IR}\mathbf{q}_R\right) \tag{2.3}$$

This leads to

$$\begin{bmatrix} \tilde{\mathbf{D}}_{LL} - \tilde{\mathbf{D}}_{LI}\tilde{\mathbf{D}}_{II}^{-1}\tilde{\mathbf{D}}_{IL} & \tilde{\mathbf{D}}_{LR} - \tilde{\mathbf{D}}_{LI}\tilde{\mathbf{D}}_{II}^{-1}\tilde{\mathbf{D}}_{IR} \\ \tilde{\mathbf{D}}_{RL} - \tilde{\mathbf{D}}_{RI}\tilde{\mathbf{D}}_{II}^{-1}\tilde{\mathbf{D}}_{IL} & \tilde{\mathbf{D}}_{RR} - \tilde{\mathbf{D}}_{RI}\tilde{\mathbf{D}}_{II}^{-1}\tilde{\mathbf{D}}_{IR} \end{bmatrix} \begin{bmatrix} \mathbf{q}_L \\ \mathbf{q}_R \end{bmatrix} = \begin{bmatrix} \mathbf{f}_L \\ \mathbf{f}_R \end{bmatrix} \tag{2.4}$$

which, in the following, will be written as

$$\begin{bmatrix} \mathbf{D}_{LL} & \mathbf{D}_{LR} \\ \mathbf{D}_{RL} & \mathbf{D}_{RR} \end{bmatrix} \begin{bmatrix} \mathbf{q}_L \\ \mathbf{q}_R \end{bmatrix} = \begin{bmatrix} \mathbf{f}_L \\ \mathbf{f}_R \end{bmatrix} \tag{2.5}$$

The new dynamic stiffness matrix is thus obtained after elimination of the interior degrees of freedom. By symmetry of the stiffness, damping and mass matrices, the dynamic stiffness matrix is also symmetric, which leads to ${}^t\mathbf{D}_{LL} = \mathbf{D}_{LL}$, ${}^t\mathbf{D}_{RR} = \mathbf{D}_{RR}$ and ${}^t\mathbf{D}_{LR} = \mathbf{D}_{RL}$, where t indicates the transpose. Relation (2.5) linking the forces and displacements on the two sides of the cell boundary will be the starting point of the further developments.

2.2 Structure with several cells

Let us consider now a structure with N identical cells like in figure 3. The displacements at each boundary are denoted by $\mathbf{q}_i$ for $1 \le i \le N+1$. We suppose that there are only external loads at sections 1 and N+1 with the load vectors denoted by $\mathbf{f}_1$ and $\mathbf{f}_{N+1}$. We are looking for an efficient way of calculating the global dynamic stiffness matrix connecting the displacements and forces at sections 1 and N+1.

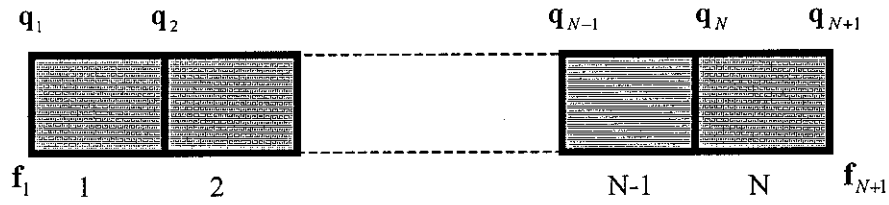

Figure 3: Structure with N cells.

Let us consider the global dynamic stiffness matrix obtained from assembling the elementary stiffness matrices from cells 1 to N. It is given by

$$\mathbf{D}_T = \begin{bmatrix} \mathbf{D}_{LL} & \mathbf{D}_{LR} & 0 & \cdots & 0 & 0 & 0 & \cdots & 0 & 0 & 0 \\ \mathbf{D}_{RL} & \mathbf{D}_{LL}+\mathbf{D}_{RR} & \mathbf{D}_{LR} & \cdots & 0 & 0 & 0 & \cdots & 0 & 0 & 0 \\ \vdots & \vdots & \vdots & \cdots & \vdots & \vdots & \vdots & \cdots & \vdots & \vdots & \vdots \\ 0 & 0 & 0 & \cdots & \mathbf{D}_{RL} & \mathbf{D}_{LL}+\mathbf{D}_{RR} & \mathbf{D}_{LR} & \cdots & 0 & 0 & 0 \\ \vdots & \vdots & \vdots & \cdots & \vdots & \vdots & \vdots & \cdots & \vdots & \vdots & \vdots \\ 0 & 0 & 0 & \cdots & 0 & 0 & 0 & \cdots & \mathbf{D}_{RL} & \mathbf{D}_{LL}+\mathbf{D}_{RR} & \mathbf{D}_{LR} \\ 0 & 0 & 0 & \cdots & 0 & 0 & 0 & \cdots & 0 & \mathbf{D}_{RL} & \mathbf{D}_{RR} \end{bmatrix} \tag{2.6}$$

and the relation between the displacements and forces is

$$\mathbf{D}_T \begin{bmatrix} \mathbf{q}_1 \\ \mathbf{q}_2 \\ \vdots \\ \mathbf{q}_i \\ \vdots \\ \mathbf{q}_N \\ \mathbf{q}_{N+1} \end{bmatrix} = \begin{bmatrix} \mathbf{f}_1 \\ 0 \\ \vdots \\ 0 \\ \vdots \\ 0 \\ \mathbf{f}_{N+1} \end{bmatrix} \tag{2.7}$$

It follows that for $1 < i < N+1$, one has the recurrence relation for the displacement vectors

$$\mathbf{D}_{RL}\mathbf{q}_{i-1} + (\mathbf{D}_{LL} + \mathbf{D}_{RR})\mathbf{q}_i + \mathbf{D}_{LR}\mathbf{q}_{i+1} = 0 \tag{2.8}$$

Let us introduce now the left and right propagation matrices, $\mathbf{P}_l$ and $\mathbf{P}_r$, which are defined by

$$\begin{aligned} \mathbf{D}_{RL}\mathbf{P}_l^2 + (\mathbf{D}_{LL} + \mathbf{D}_{RR})\mathbf{P}_l + \mathbf{D}_{LR} = 0 \\ \mathbf{D}_{RL} + (\mathbf{D}_{LL} + \mathbf{D}_{RR})\mathbf{P}_r + \mathbf{D}_{LR}\mathbf{P}_r^2 = 0 \end{aligned} \tag{2.9}$$

with the further constraint that these matrices have only eigenvalues of modulus less than or equal to one. This constraint is added to assure that $\mathbf{P}_l^n$ and $\mathbf{P}_r^n$ are bounded matrices for any positive number n. We will see in the following how these matrices can be built. Now the solution of equation (2.8) can be written in the form

$$\mathbf{q}_i = \mathbf{P}_r^{i-1}\mathbf{u}_1 + \mathbf{P}_l^{N+1-i}\mathbf{u}_2 \tag{2.10}$$

The vectors $\mathbf{u}_1$ and $\mathbf{u}_2$ can be calculated from the displacements at sections 1 and $N+1$ by solving:

$$\begin{aligned} \mathbf{q}_1 = \mathbf{u}_1 + \mathbf{P}_l^N\mathbf{u}_2 \\ \mathbf{q}_{N+1} = \mathbf{P}_r^N\mathbf{u}_1 + \mathbf{u}_2 \end{aligned} \tag{2.11}$$

which gives

$$\begin{aligned} \mathbf{u}_1 = \left[\mathbf{I} - \mathbf{P}_l^N\mathbf{P}_r^N\right]^{-1}\left(\mathbf{q}_1 - \mathbf{P}_l^N\mathbf{q}_{N+1}\right) \\ \mathbf{u}_2 = \left[\mathbf{I} - \mathbf{P}_r^N\mathbf{P}_l^N\right]^{-1}\left(-\mathbf{P}_r^N\mathbf{q}_1 + \mathbf{q}_{N+1}\right) \end{aligned} \tag{2.12}$$

After some simple transformations, this leads to

$$\mathbf{q}_i = \left(\mathbf{P}_r^{i-1} - \mathbf{P}_l^{N+1-i}\mathbf{P}_r^N\right)\left[\mathbf{I} - \mathbf{P}_l^N\mathbf{P}_r^N\right]^{-1}\mathbf{q}_1 + \left(-\mathbf{P}_r^{i-1}\mathbf{P}_l^N + \mathbf{P}_l^{N+1-i}\right)\left[\mathbf{I} - \mathbf{P}_r^N\mathbf{P}_l^N\right]^{-1}\mathbf{q}_{N+1} \tag{2.13}$$

It can be verified that the solution given by (2.10) satisfies relation (2.7) for the sections $1 < i < N+1$ and, in fact, for any vectors $\mathbf{u}_1$ and $\mathbf{u}_2$. To complete the calculation, we also have two further relations for sections 1 and $N+1$ giving

$$\begin{aligned} \mathbf{f}_1 = \mathbf{D}_{LL}\mathbf{q}_1 + \mathbf{D}_{LR}\mathbf{q}_2 \\ \mathbf{f}_{N+1} = \mathbf{D}_{RL}\mathbf{q}_N + \mathbf{D}_{RR}\mathbf{q}_{N+1} \end{aligned} \tag{2.14}$$

If we write $\mathbf{q}_2$ and $\mathbf{q}_N$ in terms of $\mathbf{u}_1$ and $\mathbf{u}_2$ using (2.10) and, then, in terms of $\mathbf{q}_1$ and $\mathbf{q}_{N+1}$, using (2.12), we finally get the dynamic stiffness matrix for the whole structure. After some simplification and rearrangement, this leads to

$$\begin{bmatrix} \mathbf{f}_1 \\ \mathbf{f}_{N+1} \end{bmatrix} = \left(\begin{bmatrix} \mathbf{D}_{LL} & 0 \\ 0 & \mathbf{D}_{RR} \end{bmatrix} + \begin{bmatrix} \mathbf{D}_{LR} & 0 \\ 0 & \mathbf{D}_{RL} \end{bmatrix} \begin{bmatrix} \mathbf{P}_l^{N-1} & \mathbf{P}_r \\ \mathbf{P}_l & \mathbf{P}_r^{N-1} \end{bmatrix} \begin{bmatrix} \mathbf{P}_l^{N} & \mathbf{I} \\ \mathbf{I} & \mathbf{P}_r^{N} \end{bmatrix}^{-1} \right) \begin{bmatrix} \mathbf{q}_1 \\ \mathbf{q}_{N+1} \end{bmatrix} \quad (2.15)$$

Thus the dynamic stiffness matrix can be easily calculated when the propagation matrices are known. In the following, efficient means of calculating $\mathbf{P}_l$, $\mathbf{P}_r$ and their powers are found.

So, the starting point of this approach is the dynamic stiffness matrix of a cell of the periodic structure. The matrix can be obtained analytically for simple cases or, more generally, from standard finite element software after meshing the cell and solving a simple dynamic problem to create the mass and stiffness matrices. Then after eliminating the interior degrees of freedom, a dynamic stiffness matrix linking the forces and displacements at the left and right sides of the cell is obtained. For a periodic structure, we introduced the right and left propagation matrices, which are solutions of a recurrence equation. The global dynamic stiffness matrix of a structure with N cells is then obtained from these propagation matrices. One must notice that the calculation cost to get this global dynamic stiffness matrix does not depend on the number of cells N.

3. Wave analysis

To obtain a deeper insight into the wave propagation phenomenon in the structure and to find formulas for the propagation matrices, the structure will be analysed in terms of waves.

3.1 Transfer matrix

Continuity of displacements and equilibrium of forces at the boundary between cells n and n+1 yield, if there are no external forces applied to the structure,

$$\begin{aligned} \mathbf{q}_L^{n+1} &= \mathbf{q}_R^n \\ \mathbf{f}_L^{n+1} &= -\mathbf{f}_R^n \end{aligned} \tag{3.1}$$

We introduce the transfer matrix $\mathbf{T}$ linking the displacements and forces in cross-sections n and n+1. Using the preceding relations, this matrix is defined by

$$\mathbf{T}\begin{bmatrix} \mathbf{q}_L^n \\ \mathbf{f}_L^n \end{bmatrix} = \begin{bmatrix} \mathbf{q}_R^n \\ -\mathbf{f}_R^n \end{bmatrix} = \begin{bmatrix} \mathbf{q}_L^{n+1} \\ \mathbf{f}_L^{n+1} \end{bmatrix} \tag{3.2}$$

From the first row of relation (2.5), one gets

$$\mathbf{q}_L^{n+1} = \mathbf{D}_{LR}^{-1}\left(\mathbf{f}_L^n - \mathbf{D}_{LL}\mathbf{q}_L^n\right) \tag{3.3}$$

Introducing the preceding relation in the second row of (2.5) gives

$$\left(\mathbf{D}_{RL} - \mathbf{D}_{RR}\mathbf{D}_{LR}^{-1}\mathbf{D}_{LL}\right)\mathbf{q}_L^n + \mathbf{D}_{RR}\mathbf{D}_{LR}^{-1}\mathbf{f}_L^n = -\mathbf{f}_L^{n+1} \tag{3.4}$$

Relations (3.3) and (3.4) finally give the transfer matrix

$$\mathbf{T} = \begin{bmatrix} -\mathbf{D}_{LR}^{-1}\mathbf{D}_{LL} & \mathbf{D}_{LR}^{-1} \\ -\mathbf{D}_{RL} + \mathbf{D}_{RR}\mathbf{D}_{LR}^{-1}\mathbf{D}_{LL} & -\mathbf{D}_{RR}\mathbf{D}_{LR}^{-1} \end{bmatrix} \tag{3.5}$$

This matrix only depends on the properties of the cell n. The propagation constants and free waves are the eigenvalues and eigenvectors of this matrix defined by the eigensolutions to

$$\mathbf{T}\begin{bmatrix} \mathbf{q}_L \\ \mathbf{f}_L \end{bmatrix} = \lambda\begin{bmatrix} \mathbf{q}_L \\ \mathbf{f}_L \end{bmatrix} \tag{3.6}$$

The first row of (3.5) leads to

$$\left(\mathbf{D}_{LL} + \lambda\mathbf{D}_{LR}\right)\mathbf{q}_L = \mathbf{f}_L \tag{3.7}$$

Substituting this for the force in the second row of (3.5) gives,

$$\left(-\mathbf{D}_{RL}+\mathbf{D}_{RR}\mathbf{D}_{LR}^{-1}\mathbf{D}_{LL}\right)\mathbf{q}_L-\mathbf{D}_{RR}\mathbf{D}_{LR}^{-1}\left(\mathbf{D}_{LL}+\lambda\mathbf{D}_{LR}\right)\mathbf{q}_L=\lambda\left(\mathbf{D}_{LL}+\lambda\mathbf{D}_{LR}\right)\mathbf{q}_L \tag{3.8}$$

After simplification, this leads to the relation

$$\left(\mathbf{D}_{LL}+\mathbf{D}_{RR}+\lambda\mathbf{D}_{LR}+\frac{1}{\lambda}\mathbf{D}_{RL}\right)\mathbf{q}_L=0 \tag{3.9}$$

This relation can also be obtained from the dynamic stiffness matrix (2.5) with

$$\begin{bmatrix}\mathbf{f}_L\\ \mathbf{f}_R\end{bmatrix}=\begin{bmatrix}\mathbf{I}\\ -\lambda\mathbf{I}\end{bmatrix}\mathbf{f}_L \qquad \begin{bmatrix}\mathbf{q}_L\\ \mathbf{q}_R\end{bmatrix}=\begin{bmatrix}\mathbf{I}\\ \lambda\mathbf{I}\end{bmatrix}\mathbf{q}_L \tag{3.10}$$

and

$$\begin{bmatrix}\mathbf{I} & \frac{1}{\lambda}\mathbf{I}\end{bmatrix}\mathbf{D}\begin{bmatrix}\mathbf{I}\\ \lambda\mathbf{I}\end{bmatrix}\mathbf{q}_L=0 \tag{3.11}$$

The force component of the eigenvector is given by (3.7). An interesting property can be proved. From relation (3.9), it is clear that the eigenvalues are the roots of the determinant

$$\left|\mathbf{D}_{LL}+\mathbf{D}_{RR}+\lambda\mathbf{D}_{LR}+\frac{1}{\lambda}\mathbf{D}_{RL}\right|=0 \tag{3.12}$$

Taking the transpose of the matrix one also has

$$\left|\mathbf{D}_{LL}+\mathbf{D}_{RR}+\lambda\mathbf{D}_{RL}+\frac{1}{\lambda}\mathbf{D}_{LR}\right|=0 \tag{3.13}$$

This leads to the fundamental property that if λ is an eigenvalue, $1/\lambda$ is also an eigenvalue. This is true for any shape or property of the cell.

3.2 Wave basis

The wave modes are the eigenvectors of the transfer matrix. So the *2n* eigenvalues of (3.5) can be split into two sets of n eigenvalues and eigenvectors which are denoted by $(\lambda_i,\boldsymbol{\Phi}_i^+)$ and $(1/\lambda_i,\boldsymbol{\Phi}_i^-)$ with the first set such that $|\lambda_i|\le 1$. In the case $|\lambda_i|=1$, the first set must contain the waves propagating in the positive direction, which are such that $\mathrm{Re}\{i\omega\mathbf{q}_L^H\mathbf{f}_L\}>0$. The inverse eigenvalue $1/\lambda_i$, in the second set, is associated with the waves such that $\mathrm{Re}\{i\omega\mathbf{q}_L^H\mathbf{f}_L\}<0$. The right eigenvector for the eigenvalue λ_i is thus given by

$$\mathbf{\Phi}_i = \mathbf{\Phi}(\lambda_i) = \begin{bmatrix} \mathbf{q}(\lambda_i) \\ \mathbf{f}(\lambda_i) \end{bmatrix} = \begin{bmatrix} \mathbf{q}(\lambda_i) \\ (\mathbf{D}_{LL} + \lambda_i \mathbf{D}_{LR})\mathbf{q}(\lambda_i) \end{bmatrix} \tag{3.14}$$

It is proved in [6] that for symmetric elements and attenuating waves, the positive and negative eigenvectors are equals, that is $\mathbf{q}(\lambda_i) = \mathbf{q}(1/\lambda_i)$ if λ_i and $\mathbf{T}$ are real. In the general case there is no simple relation between these two vectors.

It can also be shown that the left eigenvectors are

$$\mathbf{\Psi}_i = \mathbf{\Psi}(\lambda_i) = \begin{bmatrix} {}^t\mathbf{q}(\frac{1}{\lambda_i})(\mathbf{D}_{RR} + \lambda_i \mathbf{D}_{LR}) & {}^t\mathbf{q}(\frac{1}{\lambda_i}) \end{bmatrix} \tag{3.15}$$

Orthogonality properties can be obtained from the following relations

$$\begin{aligned} \mathbf{T}\mathbf{\Phi}_j &= \lambda_j \mathbf{\Phi}_j \\ \mathbf{\Psi}_i \mathbf{T} &= \lambda_i \mathbf{\Psi}_i \end{aligned} \tag{3.16}$$

which leads to

$$\mathbf{\Psi}_i \mathbf{T} \mathbf{\Phi}_j = \lambda_j \mathbf{\Psi}_i \mathbf{\Phi}_j = \lambda_i \mathbf{\Psi}_i \mathbf{\Phi}_j \tag{3.17}$$

This quantity must equal zero if $\lambda_i \neq \lambda_j$. So, the left and right eigenvectors are such that

$$\mathbf{\Psi}_i \mathbf{\Phi}_j = d_i \delta_{ij} \tag{3.18}$$

A normalization of the eigenvectors could lead to $d_i = 1$, but it is better to keep the relation in the form (3.18) and to normalize the vectors $\mathbf{q}(\lambda_i)$ and $\mathbf{q}(1/\lambda_i)$.

3.3 Wave decomposition

The free waves can be written as a linear combination of the eigenvectors. So, the left state vector is given by the following sum of positive and negative waves with respective amplitudes a_i^+ and a_i^-

$$\mathbf{x}_L = \begin{bmatrix} \mathbf{q}_L \\ \mathbf{f}_L \end{bmatrix} = \sum_{i=1}^{i=n} \left(a_i^+ \mathbf{\Phi}_i^+ + a_i^- \mathbf{\Phi}_i^- \right) \tag{3.19}$$

In the same way, the right state vector is given by

$$\mathbf{x}_R = \begin{bmatrix} \mathbf{q}_R \\ -\mathbf{f}_R \end{bmatrix} = \sum_{i=1}^{i=n} \left(b_i^+ \mathbf{\Phi}_i^+ + b_i^- \mathbf{\Phi}_i^- \right) \tag{3.20}$$

The relations between the incoming and outgoing waves in the cell are obtained from $\mathbf{x}_R = \mathbf{T}\mathbf{x}_L$ and after rearrangement this gives

$$\begin{bmatrix} \mathbf{b}^+ \\ \mathbf{a}^- \end{bmatrix} = \begin{bmatrix} \mathbf{\Lambda} & 0 \\ 0 & \mathbf{\Lambda} \end{bmatrix} \begin{bmatrix} \mathbf{a}^+ \\ \mathbf{b}^- \end{bmatrix} \tag{3.21}$$

where the vectors $\mathbf{a}^+$, $\mathbf{a}^-$, $\mathbf{b}^+$ and $\mathbf{b}^-$ contain the amplitudes of the waves and the diagonal matrix $\mathbf{\Lambda} = diag(\lambda_1, \ldots, \lambda_n)$ contains the eigenvalues of modulus less than or equal to one.

From the relations (3.19) and (3.20), using the orthogonal properties (3.18), the modal amplitudes can be obtained from the left and right state vectors by the scalar products

$$\begin{aligned} d_i^+ a_i^+ &= \mathbf{\Psi}_i^+ \cdot \mathbf{x}_L \qquad & d_i^+ b_i^+ &= \mathbf{\Psi}_i^+ \cdot \mathbf{x}_R \\ d_i^- a_i^- &= \mathbf{\Psi}_i^- \cdot \mathbf{x}_L \qquad & d_i^- b_i^- &= \mathbf{\Psi}_i^- \cdot \mathbf{x}_R \end{aligned} \tag{3.22}$$

where the $d_i^{\pm}$ are the factors introduced in relation (3.18). So the relation (3.21) in the case of N cells can be written as

$$\begin{bmatrix} \mathbf{\Psi}^+ \cdot \mathbf{x}_R \\ \mathbf{\Psi}^- \cdot \mathbf{x}_L \end{bmatrix} = \begin{bmatrix} \mathbf{\Lambda}^N & 0 \\ 0 & \mathbf{\Lambda}^N \end{bmatrix} \begin{bmatrix} \mathbf{\Psi}^+ \cdot \mathbf{x}_L \\ \mathbf{\Psi}^- \cdot \mathbf{x}_R \end{bmatrix} \tag{3.23}$$

Introduce now the partition

$$\mathbf{\Psi}^+ = \begin{bmatrix} {}^t\mathbf{Q}_z^- & {}^t\mathbf{Q}^- \end{bmatrix} \qquad \mathbf{\Psi}^- = \begin{bmatrix} {}^t\mathbf{Q}_z^+ & {}^t\mathbf{Q}^+ \end{bmatrix} \tag{3.24}$$

with

$$\begin{aligned} \mathbf{Q}^+ &= \begin{bmatrix} \mathbf{q}(\lambda_1) & \cdots & \mathbf{q}(\lambda_n) \end{bmatrix} \\ \mathbf{Q}^- &= \begin{bmatrix} \mathbf{q}(\frac{1}{\lambda_1}) & \cdots & \mathbf{q}(\frac{1}{\lambda_n}) \end{bmatrix} \end{aligned} \tag{3.25}$$

and

$$\begin{aligned} {}^t\mathbf{Q}_z^+ &= {}^t\mathbf{Q}^+\mathbf{D}_{RR} + \mathbf{\Lambda}^{-1}\,{}^t\mathbf{Q}^+\mathbf{D}_{LR} = -{}^t\mathbf{Q}^+\mathbf{D}_{LL} - \mathbf{\Lambda}\,{}^t\mathbf{Q}^+\mathbf{D}_{RL} \\ {}^t\mathbf{Q}_z^- &= {}^t\mathbf{Q}^-\mathbf{D}_{RR} + \mathbf{\Lambda}\,{}^t\mathbf{Q}^-\mathbf{D}_{LR} = -{}^t\mathbf{Q}^-\mathbf{D}_{LL} - \mathbf{\Lambda}^{-1}\,{}^t\mathbf{Q}^-\mathbf{D}_{RL} \end{aligned} \tag{3.26}$$

These matrices give the force components of the left eigenvectors. The relation (3.23) can also be written as

$$\begin{bmatrix} {}^t\mathbf{Q}_z^- & {}^t\mathbf{Q}^- \\ \mathbf{\Lambda}^N\,{}^t\mathbf{Q}_z^+ & \mathbf{\Lambda}^N\,{}^t\mathbf{Q}^+ \end{bmatrix} \begin{bmatrix} \mathbf{q}_R \\ -\mathbf{f}_R \end{bmatrix} = \begin{bmatrix} \mathbf{\Lambda}^N\,{}^t\mathbf{Q}_z^- & \mathbf{\Lambda}^N\,{}^t\mathbf{Q}^- \\ {}^t\mathbf{Q}_z^+ & {}^t\mathbf{Q}^+ \end{bmatrix} \begin{bmatrix} \mathbf{q}_L \\ \mathbf{f}_L \end{bmatrix} \tag{3.27}$$

or in the form

$$\begin{bmatrix} \mathbf{\Lambda}^N\,{}^t\mathbf{Q}^- & {}^t\mathbf{Q}^- \\ {}^t\mathbf{Q}^+ & \mathbf{\Lambda}^N\,{}^t\mathbf{Q}^+ \end{bmatrix} \begin{bmatrix} \mathbf{f}_L \\ \mathbf{f}_R \end{bmatrix} = \begin{bmatrix} -\mathbf{\Lambda}^N\,{}^t\mathbf{Q}_z^- & {}^t\mathbf{Q}_z^- \\ -{}^t\mathbf{Q}_z^+ & \mathbf{\Lambda}^N\,{}^t\mathbf{Q}_z^+ \end{bmatrix} \begin{bmatrix} \mathbf{q}_L \\ \mathbf{q}_R \end{bmatrix} \tag{3.28}$$

Replacing $\mathbf{Q}_z^{\pm}$ by the expressions (3.26) gives

$$\begin{aligned}
&\begin{bmatrix} \boldsymbol{\Lambda}^N {}^t\mathbf{Q}^- & {}^t\mathbf{Q}^- \\ {}^t\mathbf{Q}^+ & \boldsymbol{\Lambda}^N {}^t\mathbf{Q}^+ \end{bmatrix} \begin{bmatrix} \mathbf{f}_L \\ \mathbf{f}_R \end{bmatrix} \\
&= \begin{bmatrix} \boldsymbol{\Lambda}^N {}^t\mathbf{Q}^-\mathbf{D}_{LL} + \boldsymbol{\Lambda}^{N-1} {}^t\mathbf{Q}^-\mathbf{D}_{RL} & {}^t\mathbf{Q}^-\mathbf{D}_{RR} + \boldsymbol{\Lambda}{}^t\mathbf{Q}^-\mathbf{D}_{LR} \\ {}^t\mathbf{Q}^+\mathbf{D}_{LL} + \boldsymbol{\Lambda}{}^t\mathbf{Q}^+\mathbf{D}_{RL} & \boldsymbol{\Lambda}^N {}^t\mathbf{Q}^+\mathbf{D}_{RR} + \boldsymbol{\Lambda}^{N-1} {}^t\mathbf{Q}^+\mathbf{D}_{LR} \end{bmatrix} \begin{bmatrix} \mathbf{q}_L \\ \mathbf{q}_R \end{bmatrix} \\
&= \begin{bmatrix} \boldsymbol{\Lambda}^N {}^t\mathbf{Q}^- & {}^t\mathbf{Q}^- \\ {}^t\mathbf{Q}^+ & \boldsymbol{\Lambda}^N {}^t\mathbf{Q}^+ \end{bmatrix} \begin{bmatrix} \mathbf{D}_{LL}\mathbf{q}_L \\ \mathbf{D}_{RR}\mathbf{q}_R \end{bmatrix} + \begin{bmatrix} \boldsymbol{\Lambda}^{N-1} {}^t\mathbf{Q}^- & \boldsymbol{\Lambda}{}^t\mathbf{Q}^- \\ \boldsymbol{\Lambda}{}^t\mathbf{Q}^+ & \boldsymbol{\Lambda}^{N-1} {}^t\mathbf{Q}^+ \end{bmatrix} \begin{bmatrix} \mathbf{D}_{RL}\mathbf{q}_L \\ \mathbf{D}_{LR}\mathbf{q}_R \end{bmatrix}
\end{aligned} \tag{3.29}$$

Multiplying by the inverse of the matrix on the left side leads to

$$\begin{aligned}
\begin{bmatrix} \mathbf{f}_L \\ \mathbf{f}_R \end{bmatrix} &= \begin{bmatrix} \mathbf{D}_{LL}\mathbf{q}_L \\ \mathbf{D}_{RR}\mathbf{q}_R \end{bmatrix} + \begin{bmatrix} \boldsymbol{\Lambda}^N {}^t\mathbf{Q}^- & {}^t\mathbf{Q}^- \\ {}^t\mathbf{Q}^+ & \boldsymbol{\Lambda}^N {}^t\mathbf{Q}^+ \end{bmatrix}^{-1} \begin{bmatrix} \boldsymbol{\Lambda}^{N-1} {}^t\mathbf{Q}^- & \boldsymbol{\Lambda}{}^t\mathbf{Q}^- \\ \boldsymbol{\Lambda}{}^t\mathbf{Q}^+ & \boldsymbol{\Lambda}^{N-1} {}^t\mathbf{Q}^+ \end{bmatrix} \begin{bmatrix} \mathbf{D}_{RL}\mathbf{q}_L \\ \mathbf{D}_{LR}\mathbf{q}_R \end{bmatrix} \\
&= \begin{bmatrix} \mathbf{D}_{LL}\mathbf{q}_L \\ \mathbf{D}_{RR}\mathbf{q}_R \end{bmatrix} + \begin{bmatrix} \mathbf{Q}_N^- & \mathbf{I} \\ \mathbf{I} & \mathbf{Q}_N^+ \end{bmatrix}^{-1} \begin{bmatrix} \mathbf{Q}_{N-1}^- & \mathbf{Q}_1^- \\ \mathbf{Q}_1^+ & \mathbf{Q}_{N-1}^+ \end{bmatrix} \begin{bmatrix} \mathbf{D}_{RL}\mathbf{q}_L \\ \mathbf{D}_{LR}\mathbf{q}_R \end{bmatrix}
\end{aligned} \tag{3.30}$$

and hence

$$\begin{bmatrix} \mathbf{f}_L \\ \mathbf{f}_R \end{bmatrix} = \left(\begin{bmatrix} \mathbf{D}_{LL} & 0 \\ 0 & \mathbf{D}_{RR} \end{bmatrix} + \begin{bmatrix} \mathbf{D}_{LR} & 0 \\ 0 & \mathbf{D}_{RL} \end{bmatrix} \begin{bmatrix} \mathbf{P}_l^{N-1} & \mathbf{P}_r \\ \mathbf{P}_l & \mathbf{P}_r^{N-1} \end{bmatrix} \begin{bmatrix} \mathbf{P}_l^N & \mathbf{I} \\ \mathbf{I} & \mathbf{P}_r^N \end{bmatrix}^{-1} \right) \begin{bmatrix} \mathbf{q}_L \\ \mathbf{q}_R \end{bmatrix} \tag{3.31}$$

with $\mathbf{Q}_i^+ = \left({}^t\mathbf{Q}^+\right)^{-1} \boldsymbol{\Lambda}^i {}^t\mathbf{Q}^+$ and $\mathbf{Q}_i^- = \left({}^t\mathbf{Q}^-\right)^{-1} \boldsymbol{\Lambda}^i {}^t\mathbf{Q}^-$. Equation (3.31) gives the dynamic stiffness matrix of the structure and is obtained from equation (3.30) by the symmetry of the dynamic stiffness matrix and the following relations

$$\begin{aligned}
\mathbf{P}_l &= \mathbf{Q}^-\boldsymbol{\Lambda}\left(\mathbf{Q}^-\right)^{-1} \\
\mathbf{P}_r &= \mathbf{Q}^+\boldsymbol{\Lambda}\left(\mathbf{Q}^+\right)^{-1}
\end{aligned} \tag{3.32}$$

It can be checked that these matrices are solutions of (2.9). We find again the formula (2.15), but now the expressions for the propagation matrices are given in term of waves and propagation constants. The matrix $\mathbf{P}_r$ is in fact the matrix with the eigenvalues λ_i and eigenvectors $\mathbf{q}(\lambda_i)$, while $\mathbf{P}_l$ has eigenvalues λ_i and eigenvectors $\mathbf{q}(1/\lambda_i)$.

3.4 Numerical calculation of wave eigenproperties

To numerically calculate the eigenvalues and eigenvectors, one has to solve the eigenvalue problem (3.6) or (3.9). For a small number of degrees of freedom, we calculate the eigenvalues and eigenvectors of the transfer matrix. For a larger number of degrees of freedom, a direct application of usual numerical solvers can lead to

difficulties because of the ill conditioning of the transfer matrix when the order of the matrix becomes large. It is better, for instance, to define a problem in term of the eigenvalue $(\lambda+1/\lambda)$ as proposed by Gry in [17] or with more mathematical details by Zhong [18], which showed that the transfer matrix is symplectic and gave a detailed analysis of its eigenvectors. This means that we look for the eigenvalues of $\mathbf{T}+\mathbf{T}^{-1}$ instead of the eigenvalues of $\mathbf{T}$. This problem can be put in the form

$$\begin{bmatrix} -\mathbf{D}_{RL} & -\mathbf{D}_{LL}-\mathbf{D}_{RR} \\ \mathbf{O} & -\mathbf{D}_{RL} \end{bmatrix}\begin{bmatrix} \mathbf{q}_L \\ \tilde{\mathbf{q}}_L \end{bmatrix} = \lambda\begin{bmatrix} \mathbf{O} & \mathbf{D}_{LR} \\ -\mathbf{D}_{RL} & \mathbf{O} \end{bmatrix}\begin{bmatrix} \mathbf{q}_L \\ \tilde{\mathbf{q}}_L \end{bmatrix} \tag{3.33}$$

where $\tilde{\mathbf{q}}_L = \lambda \mathbf{q}_L$. Another possibility is in the form

$$\begin{bmatrix} \mathbf{D}_{LR} & \mathbf{O} \\ \mathbf{D}_{LL}+\mathbf{D}_{RR} & \mathbf{D}_{LR} \end{bmatrix}\begin{bmatrix} \mathbf{q}_L \\ \tilde{\mathbf{q}}_L \end{bmatrix} = \frac{1}{\lambda}\begin{bmatrix} \mathbf{O} & \mathbf{D}_{LR} \\ -\mathbf{D}_{RL} & \mathbf{O} \end{bmatrix}\begin{bmatrix} \mathbf{q}_L \\ \tilde{\mathbf{q}}_L \end{bmatrix} \tag{3.34}$$

Taking the sum of (3.33) and (3.34) and reorganizing leads to

$$\begin{bmatrix} \mathbf{D}_{RL} & \mathbf{O} \\ \mathbf{O} & \mathbf{D}_{LR} \end{bmatrix}\begin{bmatrix} \mathbf{q}_L \\ \tilde{\mathbf{q}}_L \end{bmatrix} = \frac{1}{\lambda+\frac{1}{\lambda}}\begin{bmatrix} -(\mathbf{D}_{LL}+\mathbf{D}_{RR}) & -(\mathbf{D}_{LR}-\mathbf{D}_{RL}) \\ (\mathbf{D}_{LR}-\mathbf{D}_{RL}) & -(\mathbf{D}_{LL}+\mathbf{D}_{RR}) \end{bmatrix}\begin{bmatrix} \mathbf{q}_L \\ \tilde{\mathbf{q}}_L \end{bmatrix} \tag{3.35}$$

This last system has only double eigenvalues. Denoting two independent eigenvectors associated to the same eigenvalue as $\mathbf{w}_1$ and $\mathbf{w}_2$, an eigenvector of system (3.33) associated to the eigenvalue λ can be decomposed as:

$$\mathbf{w} = \alpha_1 \mathbf{w}_1 + \alpha_2 \mathbf{w}_2 \tag{3.36}$$

Inserting this into (3.33) gives

$$\begin{bmatrix} -\mathbf{D}_{RL} & -\mathbf{D}_{LL}-\mathbf{D}_{RR} \\ \mathbf{O} & -\mathbf{D}_{RL} \end{bmatrix}(\alpha_1\mathbf{w}_1+\alpha_2\mathbf{w}_2) = \lambda\begin{bmatrix} \mathbf{O} & \mathbf{D}_{LR} \\ -\mathbf{D}_{RL} & \mathbf{O} \end{bmatrix}(\alpha_1\mathbf{w}_1+\alpha_2\mathbf{w}_2) \tag{3.37}$$

or

$$\begin{bmatrix} -\mathbf{D}_{RL} & -\mathbf{D}_{LL}-\mathbf{D}_{RR}-\lambda\mathbf{D}_{LR} \\ \lambda\mathbf{D}_{RL} & -\mathbf{D}_{RL} \end{bmatrix}(\alpha_1\mathbf{w}_1+\alpha_2\mathbf{w}_2) = 0 \tag{3.38}$$

Taking for instance the scalar product by the complex conjugate $^*\mathbf{w}_1$, this leads to a relation between α_1 and α_2 which gives the vector $\mathbf{w}$ up to a normalization factor.

Another possibility is to use the polyeig function of matlab, which solves the polynomial eigenvalue problem. However this function does not provide clear improvement over the preceding formulation.

3.5 *Case of a symmetrical cell*

Often the cell is symmetric. This means that there exists a plane of symmetry as in figure 4. Consider the implications of symmetry on the displacements and forces leads to

$$\begin{aligned} \mathbf{q}_L^s &= \mathbf{S}\mathbf{q}_R \\ \mathbf{q}_R^s &= \mathbf{S}\mathbf{q}_L \\ \mathbf{f}_L^s &= \mathbf{S}\mathbf{f}_R \\ \mathbf{f}_R^s &= \mathbf{S}\mathbf{f}_L \end{aligned} \tag{3.39}$$

where $\mathbf{S}$ is a matrix describing the behaviour of each degree of freedom in the symmetry operation and is such that $\mathbf{S}^2 = \mathbf{I}$, the identity. For instance, the components of the displacements parallel to the plane of symmetry do not change during the symmetry while the orthogonal coordinates have their signs changed. The same is true for the components of the forces. The $\mathbf{S}$ matrix is diagonal with only 1 or –1 on the diagonal.

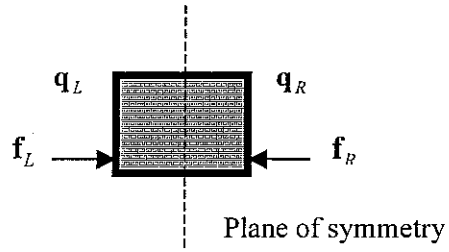

Figure 4: Symmetrical cell

Using the relations (3.39) in (2.5) leads to

$$\begin{bmatrix} \mathbf{D}_{LL} & \mathbf{D}_{LR} \\ \mathbf{D}_{RL} & \mathbf{D}_{RR} \end{bmatrix} \begin{bmatrix} \mathbf{q}_L^s \\ \mathbf{q}_R^s \end{bmatrix} = \begin{bmatrix} \mathbf{f}_L^s \\ \mathbf{f}_R^s \end{bmatrix} \tag{3.40}$$

or

$$\begin{bmatrix} \mathbf{D}_{LL} & \mathbf{D}_{LR} \\ \mathbf{D}_{RL} & \mathbf{D}_{RR} \end{bmatrix} \begin{bmatrix} \mathbf{S}\mathbf{q}_R \\ \mathbf{S}\mathbf{q}_L \end{bmatrix} = \begin{bmatrix} \mathbf{S}\mathbf{f}_R \\ \mathbf{S}\mathbf{f}_L \end{bmatrix} \tag{3.41}$$

which can be rearranged as

$$\begin{bmatrix} \mathbf{S}\mathbf{D}_{RR}\mathbf{S} & \mathbf{S}\mathbf{D}_{RL}\mathbf{S} \\ \mathbf{S}\mathbf{D}_{LR}\mathbf{S} & \mathbf{S}\mathbf{D}_{LL}\mathbf{S} \end{bmatrix} \begin{bmatrix} \mathbf{q}_L \\ \mathbf{q}_R \end{bmatrix} = \begin{bmatrix} \mathbf{f}_L \\ \mathbf{f}_R \end{bmatrix} \tag{3.42}$$

This relation must be the same as the original relation given by (2.5). So the submatrices satisfy the following symmetry relations

$$\begin{aligned}\mathbf{D}_{LL} &= \mathbf{S}\mathbf{D}_{RR}\mathbf{S}\\ \mathbf{D}_{LR} &= \mathbf{S}\mathbf{D}_{RL}\mathbf{S}\\ \mathbf{D}_{RL} &= \mathbf{S}\mathbf{D}_{LR}\mathbf{S}\\ \mathbf{D}_{RR} &= \mathbf{S}\mathbf{D}_{LL}\mathbf{S}\end{aligned} \tag{3.43}$$

Then the displacement components of an eigenvector are solution of

$$\begin{aligned}\left(\mathbf{D}_{LL}+\mathbf{D}_{RR}+\lambda\mathbf{D}_{LR}+\frac{1}{\lambda}\mathbf{D}_{RL}\right)\mathbf{q}_L &= 0\\ \left(\mathbf{S}\mathbf{D}_{RR}\mathbf{S}+\mathbf{S}\mathbf{D}_{LL}\mathbf{S}+\lambda\mathbf{S}\mathbf{D}_{RL}\mathbf{S}+\frac{1}{\lambda}\mathbf{S}\mathbf{D}_{LR}\mathbf{S}\right)\mathbf{q}_L &= 0\\ \left(\mathbf{D}_{RR}+\mathbf{D}_{LL}+\lambda\mathbf{D}_{RL}+\frac{1}{\lambda}\mathbf{D}_{LR}\right)\mathbf{S}\mathbf{q}_L &= 0\end{aligned} \tag{3.44}$$

The last relation means that the eigenvector associated with $1/\lambda$ is the symmetric partner of the eigenvector associated with λ, that is $\mathbf{q}(1/\lambda)=\mathbf{S}\mathbf{q}(\lambda)$. The full left eigenvector is

$$\begin{aligned}\mathbf{\Psi}(\lambda_i) &= \left[{}^t\mathbf{q}(\frac{1}{\lambda_i})\left(\mathbf{D}_{RR}+\lambda_i\mathbf{D}_{LR}\right)\quad {}^t\mathbf{q}(\frac{1}{\lambda_i})\right]\\ &= \left[{}^t\mathbf{q}(\lambda_i)\mathbf{S}\left(\mathbf{D}_{RR}+\lambda_i\mathbf{D}_{LR}\right)\quad {}^t\mathbf{q}(\lambda_i)\mathbf{S}\right]\\ &= \left[{}^t\mathbf{q}(\lambda_i)\left(\mathbf{D}_{LL}+\lambda_i\mathbf{D}_{RL}\right)\quad {}^t\mathbf{q}(\lambda_i)\right]\mathbf{S}\\ &= \left[-{}^t\mathbf{q}(\lambda_i)\left(\mathbf{D}_{RR}+\frac{1}{\lambda_i}\mathbf{D}_{LR}\right)\quad {}^t\mathbf{q}(\lambda_i)\right]\mathbf{S}\\ &= \mathbf{\Psi}(\frac{1}{\lambda_i})\overline{\mathbf{S}}\end{aligned} \tag{3.45}$$

where the action of the operator $\overline{\mathbf{S}}$ consists in multiplying the force and displacement components by $\mathbf{S}$ and changing the sign of the force component. The same transformation can be applied to the right eigenvectors $\mathbf{\Phi}(\lambda_i)$.

3.6 Perturbation analysis

The eigenvalues and eigenvectors are solutions of system (3.6). If we take the derivative of this relation with frequency, we get

$$\mathbf{T}'\mathbf{\Phi}_i+\mathbf{T}\mathbf{\Phi}'_i=\lambda'_i\,\mathbf{\Phi}_i+\lambda_i\mathbf{\Phi}'_i \tag{3.46}$$

Taking the product with the left eigenvector $\mathbf{\Psi}_i$ and simplifying leads to the expression for the derivative of the eigenvalue (if $\mathbf{\Psi}_j\mathbf{\Phi}_i=\delta_{ij}$)

$$\lambda'_i=\mathbf{\Psi}_i\mathbf{T}'\mathbf{\Phi}_i \tag{3.47}$$

Recalling that $\lambda = e^{ikl}$, we find that the derivative of the wavenumber is given by

$$\frac{\partial k_i}{\partial \omega} = k'_i = \frac{1}{il\lambda_i} \boldsymbol{\Psi}_i \mathbf{T}' \boldsymbol{\Phi}_i \tag{3.48}$$

Other formulas can be obtained for the derivatives of the eigenvectors. Taking the products of (3.46) with the left eigenvector $\boldsymbol{\Psi}_j$ for $j \neq i$ leads to

$$\begin{aligned} \boldsymbol{\Psi}_j \mathbf{T}' \boldsymbol{\Phi}_i + \boldsymbol{\Psi}_j \mathbf{T} \boldsymbol{\Phi}'_i &= \lambda'_i \, \boldsymbol{\Psi}_j \boldsymbol{\Phi}_i + \lambda_i \boldsymbol{\Psi}_j \boldsymbol{\Phi}'_i \\ \boldsymbol{\Psi}_j \mathbf{T}' \boldsymbol{\Phi}_i + \lambda_j \boldsymbol{\Psi}_j \boldsymbol{\Phi}'_i &= \lambda_i \boldsymbol{\Psi}_j \boldsymbol{\Phi}'_i \\ \boldsymbol{\Psi}_j \boldsymbol{\Phi}'_i &= \frac{1}{\lambda_i - \lambda_j} \boldsymbol{\Psi}_j \mathbf{T}' \boldsymbol{\Phi}_i \end{aligned} \tag{3.49}$$

The last relation gives the projection of the vectors $\boldsymbol{\Phi}'_i$ along the eigenvectors $\boldsymbol{\Phi}_j$ for $j \neq i$. As the normalization of the vector $\boldsymbol{\Phi}_i$ is arbitrary the component of $\boldsymbol{\Phi}'_i$ along $\boldsymbol{\Phi}_i$ can be arbitrarily chosen, for instance equal to zero. The matrix of the left eigenvectors satisfies

$$\boldsymbol{\Psi}\boldsymbol{\Phi} = \mathbf{I} \tag{3.50}$$

The derivative gives

$$\boldsymbol{\Psi}'\boldsymbol{\Phi} + \boldsymbol{\Psi}\boldsymbol{\Phi}' = 0 \tag{3.51}$$

So the matrix of the derivatives of the left eigenvectors is

$$\boldsymbol{\Psi}' = -\boldsymbol{\Psi}\boldsymbol{\Phi}'\boldsymbol{\Phi}^{-1} \tag{3.52}$$

The preceding calculations require the derivative of the transfer matrix. It is given by

$$\mathbf{T}' = \begin{bmatrix} \mathbf{D}_{LR}^{-1}\mathbf{D}'_{LR}\,\mathbf{D}_{LR}^{-1}\mathbf{D}_{LL} - \mathbf{D}_{LR}^{-1}\mathbf{D}'_{LL} & -\mathbf{D}_{LR}^{-1}\mathbf{D}'_{LR}\,\mathbf{D}_{LR}^{-1} \\ -\mathbf{D}'_{RL} + \mathbf{D}'_{RR}\,\mathbf{D}_{LR}^{-1}\mathbf{D}_{LL} - \mathbf{D}_{RR}\mathbf{D}_{LR}^{-1}\mathbf{D}'_{LR}\,\mathbf{D}_{LR}^{-1}\mathbf{D}_{LL} + \mathbf{D}_{RR}\mathbf{D}_{LR}^{-1}\mathbf{D}'_{LL} & -\mathbf{D}'_{RR}\,\mathbf{D}_{LR}^{-1} + \mathbf{D}_{RR}\mathbf{D}_{LR}^{-1}\mathbf{D}'_{LR}\,\mathbf{D}_{LR}^{-1} \end{bmatrix} \tag{3.53}$$

In practise, it might be neater to find $\frac{\partial}{\partial(\omega^2)} = \frac{1}{2\omega}\frac{\partial}{\partial\omega}$ when the dynamic stiffness matrix depends only on ω^2, for instance in case of hysteretic damping or without damping.

The transfer matrix, linking the displacements and forces on both sides of a cell, was introduced in this section. Then, the propagation constants and the wave basis are respectively the eigenvalues and eigenvectors of the transfer matrix. This basis allows decomposing the state vector, made of the displacements and forces in a section, into wave amplitudes. Thus, the behaviour of a structure with N cells can be written in a simple way in terms of wave amplitudes and, after some transformations, the dynamic stiffness matrix of the global structure is obtained. This also gives formulas to

calculate the propagation matrices introduced in the preceding section. Finally, some special points related to the solution of the eigenvalue problem, to the case of a symmetric structure or to the derivatives of the propagation constants and of the wave basis vectors are also analysed.

4. Results

4.1 Rod example

4.1.1 Transfer matrix

We consider first the very simple example presented in Figure 5 where a rod fixed on the left side is submitted to a force F on the right side. For this example we will give explicit calculations of all the matrices and vectors introduced in the theoretical part of the paper.

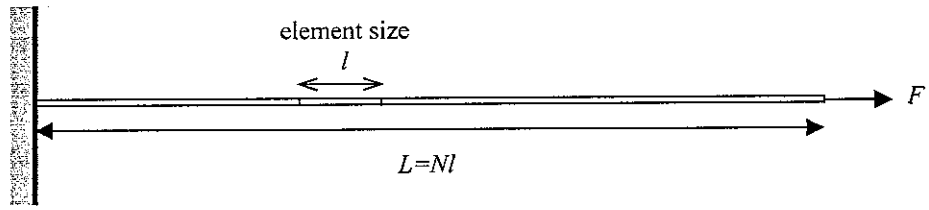

Figure 5: Rod structure

The rod is of length L and the mesh is divided into N elements of length l, such that $L=Nl$. Here N needs not be integral. The rod element with two degrees of freedom is presented in figure 6. This is our basic cell introduced in the first part of the paper.

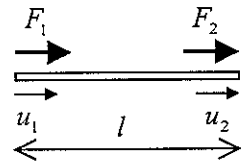

Figure 6: Rod element

The elementary stiffness and mass matrices for this element are given by (see for instance Petyt [19])

$$\mathbf{K}_e = \frac{ES}{l}\begin{bmatrix} 1 & -1 \\ -1 & 1 \end{bmatrix} \qquad \mathbf{M}_e = \frac{\rho Sl}{6}\begin{bmatrix} 2 & 1 \\ 1 & 2 \end{bmatrix} \tag{4.1}$$

where E is the Young's modulus, ρ the density of the material and S the cross-sectional area. As an example we assume hysteretic damping leading to the damping matrix $\mathbf{C}_e = \eta\mathbf{K}_e$, but the following is true for any damping model for which the function $E(\omega)$ giving the dependency of the complex Young's modulus with the frequency is known. The dynamic stiffness matrix of the element at the frequency ω is then $\mathbf{D}_e = \mathbf{K}_e + \mathbf{C}_e - \omega^2\mathbf{M}_e$. It will be more convenient to work with non dimensional quantities. Thus the displacements are written in units of l and the force in units of $\tilde{E}S$, where $\tilde{E} = (1+i\eta)E$. This leads to the following dynamic stiffness matrix

$$\mathbf{D}_e = \begin{bmatrix} 1-\frac{\rho l^2\omega^2}{3\tilde{E}} & -1-\frac{\rho l^2\omega^2}{6\tilde{E}} \\ -1-\frac{\rho l^2\omega^2}{6\tilde{E}} & 1-\frac{\rho l^2\omega^2}{3\tilde{E}} \end{bmatrix} = \begin{bmatrix} 1-\frac{(kl)^2}{3} & -1-\frac{(kl)^2}{6} \\ -1-\frac{(kl)^2}{6} & 1-\frac{(kl)^2}{3} \end{bmatrix} \tag{4.2}$$

where $k = \sqrt{\frac{\rho\omega^2}{\tilde{E}}}$ is the usual wavenumber with damping. After some simple calculations, we get the transfer matrix

$$\mathbf{T} = \frac{1}{1+\frac{(kl)^2}{6}} \begin{bmatrix} 1-\frac{(kl)^2}{3} & -1 \\ (kl)^2-\frac{(kl)^4}{12} & 1-\frac{(kl)^2}{3} \end{bmatrix} \tag{4.3}$$

Then the eigenvalues can be calculated and are given by

$$\lambda^{\pm} = \frac{1}{1+\frac{(kl)^2}{6}} \left(1-\frac{(kl)^2}{3} \pm ikl\sqrt{1-\frac{(kl)^2}{12}} \right) = 1 \pm ikl - \frac{(kl)^2}{2} + O((kl)^3) \tag{4.4}$$

For small values of *kl*, the eigenvalues are equal to $e^{\pm ikl}$ to the second order in *kl*, with the error being $O((kl)^3)$. Furthermore $|\lambda^+| = |\lambda^-| = 1$ if $(kl)^2 < 12$ and there is no damping.

4.1.2 Dispersion relations

Dispersion relations can be obtained by plotting the curves $k^{\pm}(\omega)l = \log(\lambda^{\pm}(\omega))$. In the case of no damping ($\eta = 0$), the results are given in figures 7 and 8 as function of kl and are also compared to the analytical solution. There is one coupling DOF and hence one pair of eigenvalues, which represent propagating waves below the cut-off frequency for the FE model at $kl = \sqrt{12}$. We can see that the FE predictions are smooth and waves propagate freely if $kl < \sqrt{12}$. They are close to the analytical relations for a rod for small frequencies, approximately until $kl \approx 1$. For $kl > \sqrt{12}$, the finite element model predicts a pair of attenuating waves.

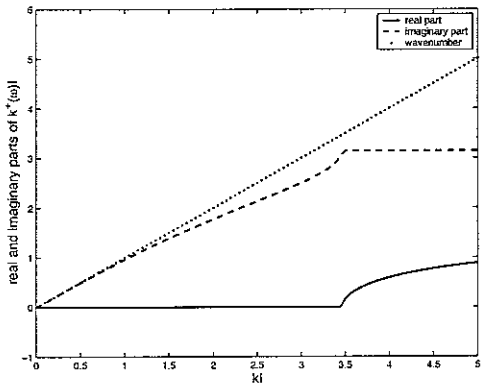

Figure 7: Dispersion relations for $k^+(\omega)$.

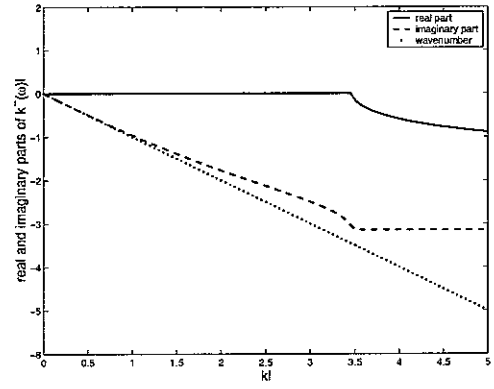

Figure 8: Dispersion relations for $k^-(\omega)$.

4.1.3 Frequency response

Next, we calculate the frequency response function (FRF) for the excitation by the force F at the right end of the rod. Following the method presented above, we need first the right and left eigenvectors. The right eigenvectors of the transfer matrix **T** are

$$\mathbf{\Phi}^{\pm} = \begin{bmatrix} \mp \dfrac{1}{\sqrt{2}ikl\sqrt{1-\dfrac{(kl)^2}{12}}} \\ \dfrac{1}{\sqrt{2}} \end{bmatrix} \tag{4.5}$$

and the left eigenvectors are

$$\mathbf{\Psi}^{\pm} = \begin{bmatrix} \mp \dfrac{ikl}{\sqrt{2}}\sqrt{1-\dfrac{(kl)^2}{12}} & \dfrac{1}{\sqrt{2}} \end{bmatrix} \tag{4.6}$$

The normalization of the right eigenvectors is arbitrary. The normalization of the left eigenvectors is chosen to satisfy the orthogonality relations of equation (3.18) with $d_i = 1$. One also sees that we have to choose $kl < \sqrt{12} \approx 3.5$ to avoid problems. In term of wavelength this means $l < 0.55\lambda$. Otherwise the transfer matrix is not necessarily diagonalisable and the eigenvectors cannot be properly defined. This is not a real issue, as we know that for a correct mesh, the element size must be less than a fraction of the wavelength, for instance $l < \lambda/5$. Thus, in practise, the length of the cell will be limited well below $kl = \sqrt{12}$ by the requirements on the accuracy of the solution. It can also be noticed that the introduction of the damping leads to well-defined eigenvectors. Ill-conditioning can be expected near $kl = \sqrt{12}$ for small damping.

Since there is just one coupling DOF, the matrices $\mathbf{Q}^-$ and $\mathbf{Q}^+$ are scalars and are given by

$$\mathbf{Q}^+ = \mathbf{Q}^- = \begin{bmatrix} \frac{1}{\sqrt{2}} \end{bmatrix} \tag{4.7}$$

and the matrices $\mathbf{P}_l$ and $\mathbf{P}_r$ are scalars, are equal and equal the eigenvalue of modulus less than or equal to one.

The relation between the forces and the displacements for a structure with N elements is, as given previously in (2.15),

$$\begin{bmatrix} \mathbf{f}_L \\ \mathbf{f}_R \end{bmatrix} = \left(\begin{bmatrix} \mathbf{D}_{LL} & 0 \\ 0 & \mathbf{D}_{RR} \end{bmatrix} + \begin{bmatrix} \mathbf{D}_{LR} & 0 \\ 0 & \mathbf{D}_{RL} \end{bmatrix} \begin{bmatrix} \mathbf{P}_l^{N-1} & \mathbf{P}_r \\ \mathbf{P}_l & \mathbf{P}_r^{N-1} \end{bmatrix} \begin{bmatrix} \mathbf{P}_l^N & \mathbf{I} \\ \mathbf{I} & \mathbf{P}_r^N \end{bmatrix}^{-1} \right) \begin{bmatrix} \mathbf{q}_L \\ \mathbf{q}_R \end{bmatrix} \tag{4.8}$$

The previous relation can also be written as

$$\begin{bmatrix} \mathbf{f}_L \\ \mathbf{f}_R \end{bmatrix} = \begin{bmatrix} \overline{\mathbf{D}}_{LL} & \overline{\mathbf{D}}_{LR} \\ \overline{\mathbf{D}}_{RL} & \overline{\mathbf{D}}_{RR} \end{bmatrix} \begin{bmatrix} \mathbf{q}_L \\ \mathbf{q}_R \end{bmatrix} \tag{4.9}$$

where the overbar means the dynamic stiffness matrix of the whole structure. As the left end is fixed $\mathbf{q}_L = 0$ and we finally get

$$\mathbf{q}_R = \left(\overline{\mathbf{D}}_{RR}\right)^{-1} \mathbf{f}_R \tag{4.10}$$

The displacement at the right end, in usual units, is obtained after some calculations

$$q_R = \frac{\left(\lambda^+\right)^N - \left(\lambda^+\right)^{-N}}{ik\sqrt{1 - \frac{(kl)^2}{12}\left(\left(\lambda^+\right)^N + \left(\lambda^+\right)^{-N}\right)}} \frac{F}{\widetilde{E}S} = \frac{\tan(kL)}{k} \frac{F}{\widetilde{E}S} + O((kl)^2) \tag{4.11}$$

The analytical solution is given by

$$u(x) = \frac{F}{k\widetilde{S}\widetilde{E}} \frac{\sin(kx)}{\cos(kL)} \tag{4.12}$$

Hence the FE/waveguide solution is accurate to order $(kl)^2$ and is hence accurate as long as kl is small. Figures 9 to 11 show analytical and numerical solutions for rods with 5, 25 and 100 elements. The normalized displacement q/l is plotted against kl. Hysteretic damping with $\eta = 0.01$ is used. The results show that the accuracy doesn't depend on the number of elements but only on the value of kl. For results with good accuracy, one should choose $kl<0.5$. The results are also compared with modal summation obtained by Ansys. The waveguide results seem more accurate in the three cases.

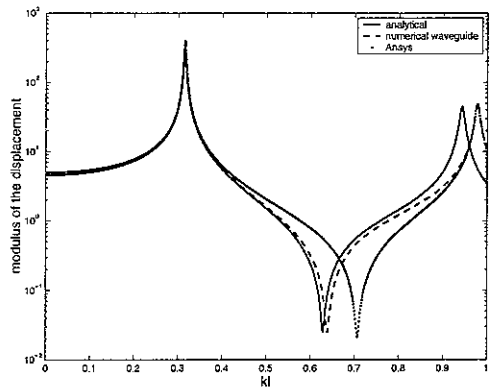

Figure 9: FRF for 5 elements.

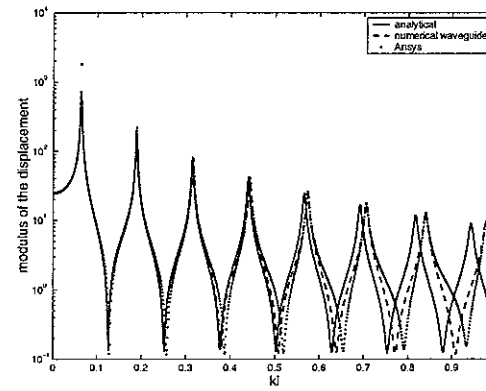

Figure 10: FRF for 25 elements.

In figure 12 is presented the FRF obtained with mass and stiffness matrices obtained from Ansys instead of using the analytical matrices of relation (4.1). In this example, the cell is made of steel with $E = 2.10^{11} Pa$, $\rho = 7800\ kg/m^3$, $l = 0.02m$ and $S = 10^{-4} m^2$. There are 100 elements. The results still agree with the analytical solution.

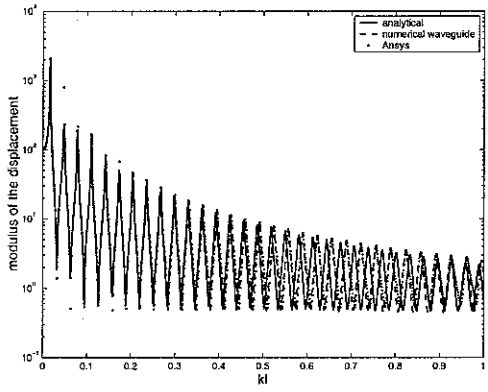

Figure 11: FRF for 100 elements.

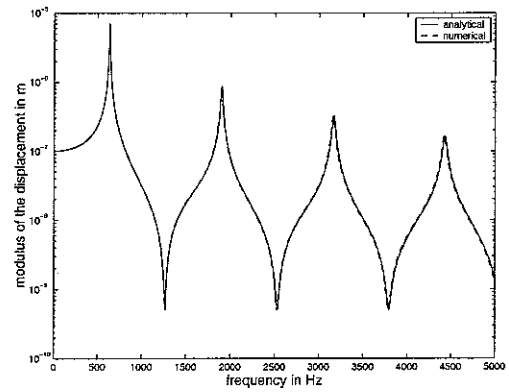

Figure 12: FRF with the matrices of Ansys.

4.2 Beam example

4.2.1 Transfer matrix

We consider now the example of the beam presented in Figure 13, which is fixed on the left side and simply supported on the right side. A force F is applied at 2/(3L).

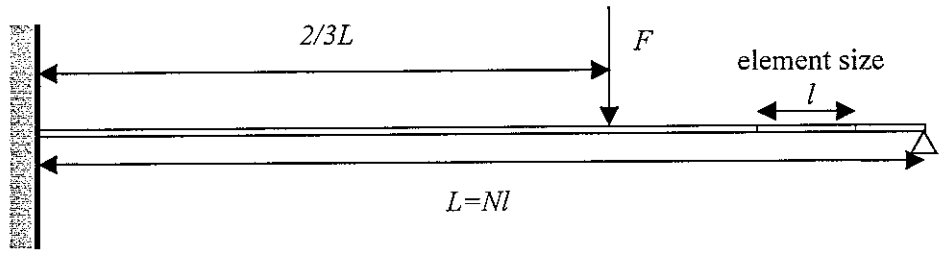

Figure 13: Beam structure

The beam is of length L and the mesh is divided into N elements of length l, such that $L=Nl$. The beam of length L is divided into two regions of lengths L_1 and L_2 by the force F. A section of length l is analysed. Then $L_1 = N_1 l$, $L_2 = N_2 l$ and N_1 and N_2 need not be integers. The beam element with four degrees of freedom is presented in figure 14. This is our basic cell introduced in the first part of the paper.

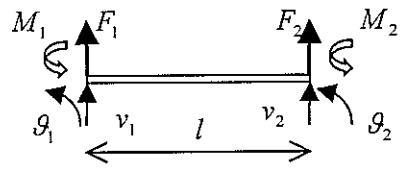

Figure 14: Beam element

The elementary stiffness and mass matrices for this element are given by (see for instance Petyt [19])

$$\mathbf{K}_e = \frac{EI}{l^3}\begin{bmatrix} 12 & 6l & -12 & 6l \\ 6l & 4l^2 & -6l & 2l^2 \\ -12 & -6l & 12 & -6l \\ 6l & 2l^2 & -6l & 4l^2 \end{bmatrix} \quad \mathbf{M}_e = \frac{\rho Sl}{420}\begin{bmatrix} 156 & 22l & 54 & -13l \\ 22l & 4l^2 & 13l & -3l^2 \\ 54 & 13l & 156 & -22l \\ -13l & -3l^2 & -22l & 4l^2 \end{bmatrix} \tag{4.13}$$

where E is the Young's modulus, ρ the density of the material, I the second moment of area and S the cross-sectional area. The damping is the same as for the rod. It is still more convenient to work with non dimensional quantities. So the displacements are written in units of l, the force in units of $\tilde{E}I/l^2$ and the momentum in units of $\tilde{E}I/l$. The dynamic stiffness matrix is now

$$\mathbf{D}_e = \begin{bmatrix} 12-\frac{156}{420}(kl)^2 & 6-\frac{22}{420}(kl)^2 & -12-\frac{54}{420}(kl)^2 & 6+\frac{13}{420}(kl)^2 \\ 6-\frac{22}{420}(kl)^2 & 4-\frac{4}{420}(kl)^2 & -6-\frac{13}{420}(kl)^2 & 2+\frac{3}{420}(kl)^2 \\ -12-\frac{54}{420}(kl)^2 & -6-\frac{13}{420}(kl)^2 & 12-\frac{156}{420}(kl)^2 & -6+\frac{22}{420}(kl)^2 \\ 6+\frac{13}{420}(kl)^2 & 2+\frac{3}{420}(kl)^2 & -6+\frac{22}{420}(kl)^2 & 4-\frac{4}{420}(kl)^2 \end{bmatrix} \tag{4.14}$$

where $k = \sqrt{\frac{\rho S l^2 \omega^2}{\tilde{E}I}}$ is a wavenumber. After some calculations, we get the transfer matrix

$$\mathbf{T} = \frac{1}{302400 + 720(kl)^2 + (kl)^4} \begin{bmatrix} 302400 + 13320(kl)^2 + 26(kl)^4 & 50400 + 180(kl)^2 \\ 50400(kl)^2 + 120(kl)^4 & 302400 + 13320(kl)^2 + 10(kl)^4 \\ 302400(kl)^2 + 2820(kl)^4 + \frac{7}{2}(kl)^6 & 151200 + 780(kl)^2 \\ -151200(kl)^2 - 570(kl)^4 - \frac{1}{4}(kl)^6 & 302400 + 13320(kl)^2 + 26(kl)^4 \\ 302400 + 3240(kl)^2 + 2(kl)^4 & -151200 - 780(kl)^2 \\ 302400 + 13320(kl)^2 + 10(kl)^4 & -302400 - 3240(kl)^2 \\ 151200(kl)^2 + 570(kl)^4 + \frac{1}{4}(kl)^6 & -50400(kl)^2 - 120(kl)^4 \\ -50400(kl)^2 - 78(kl)^4 - \frac{1}{60}(kl)^6 & 302400 + 13320(kl)^2 + 10(kl)^4 \end{bmatrix} \tag{4.15}$$

Then the eigenvalues can be calculated. Their expressions are complicated, and only the first terms of the series are given here

$$\begin{aligned} \lambda_1(kl) &= 1 + \sqrt{kl} + \frac{1}{2}kl + \frac{1}{6}(kl)^{3/2} + \frac{1}{24}(kl)^2 + O((kl)^{5/2}) \\ \lambda_2(kl) &= 1 - \sqrt{kl} + \frac{1}{2}kl - \frac{1}{6}(kl)^{3/2} + \frac{1}{24}(kl)^2 + O((kl)^{5/2}) \\ \lambda_3(kl) &= 1 + i\sqrt{kl} - \frac{1}{2}kl - \frac{i}{6}(kl)^{3/2} + \frac{1}{24}(kl)^2 + O((kl)^{5/2}) \\ \lambda_4(kl) &= 1 - i\sqrt{kl} - \frac{1}{2}kl + \frac{i}{6}(kl)^{3/2} + \frac{1}{24}(kl)^2 + O((kl)^{5/2}) \end{aligned} \tag{4.16}$$

In the above $\sqrt{kl} = \sqrt{\sqrt{\frac{\rho S l^2 \omega^2}{\tilde{E}I}}\, l} = Kl$ with $K = \sqrt[4]{\frac{\rho S \omega^2}{\tilde{E}I}}$, which is the usual wavenumber for a beam. So for small values of kl, the eigenvalues are the analytical expressions $e^{\pm Kl}$ and $e^{\pm iKl}$ accurate to the fourth order in Kl. Another possibility way to calculate the eigenvalues is to write the reduced system as

$$\left(\mathbf{D}_{LL} + \mathbf{D}_{RR} + \lambda \mathbf{D}_{LR} + \frac{1}{\lambda}\mathbf{D}_{RL}\right)\mathbf{q}_L = 0 \tag{4.17}$$

which in terms of coefficients is

$$\begin{bmatrix} 24-\frac{312}{420}(kl)^2 & 0 \\ 0 & 8-\frac{8}{420}(kl)^2 \end{bmatrix} + \lambda \begin{bmatrix} -12-\frac{54}{420}(kl)^2 & 6+\frac{13}{420}(kl)^2 \\ -6-\frac{13}{420}(kl)^2 & 2+\frac{3}{420}(kl)^2 \end{bmatrix} + \frac{1}{\lambda}\begin{bmatrix} -12-\frac{54}{420}(kl)^2 & -6-\frac{13}{420}(kl)^2 \\ 6+\frac{13}{420}(kl)^2 & 2+\frac{3}{420}(kl)^2 \end{bmatrix} = 0 \tag{4.18}$$

and the eigenvalues are also the solutions of

$$49-\frac{276}{35}(kl)^2+\frac{13}{1260}(kl)^4+\left(-96-\frac{148}{35}(kl)^2-\frac{1}{175}(kl)^4\right)\cosh(\mu) + \left(48+\frac{4}{35}(kl)^2+\frac{1}{6300}(kl)^4\right)\cosh^2(\mu)=0 \tag{4.19}$$

with $2\cosh(\mu)=\lambda+\frac{1}{\lambda}$.

4.2.2 Dispersion relations

Dispersion relations can be obtained by plotting the curves $k_i(\omega)l=\log(\lambda_i(\omega))$. The results are given in figures 15 to 18 as function of $kl=\sqrt{\frac{\rho S}{\widetilde{E}I}}l^2\omega$, which is proportional to the frequency ω. In this example, we do not consider damping in the system, so $\widetilde{E}=E$. The first two eigenvalues are real and the other two are imaginary. The behaviour is the same as for the analytical expressions for the wavenumbers of a beam, which are functions of $\sqrt{\omega}$. To allow a better comparison, the analytical wavenumbers, which are given by $\pm\sqrt{kl}$ and $\pm i\sqrt{kl}$ are also shown. The difference between the two curves is small. So the present calculation is a very good approximation to the actual behaviour.

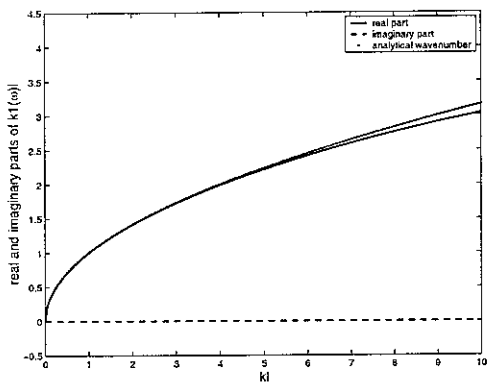

Figure 15: Dispersion relations for $k_1(\omega)$.

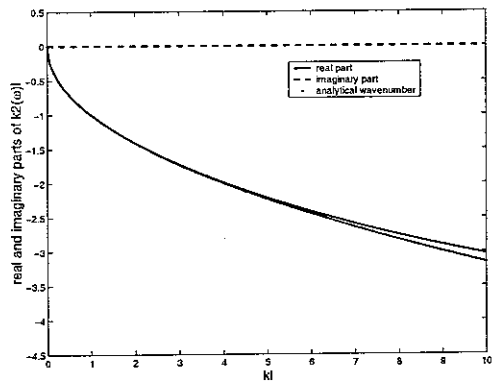

Figure 16: Dispersion relations for $k_2(\omega)$.

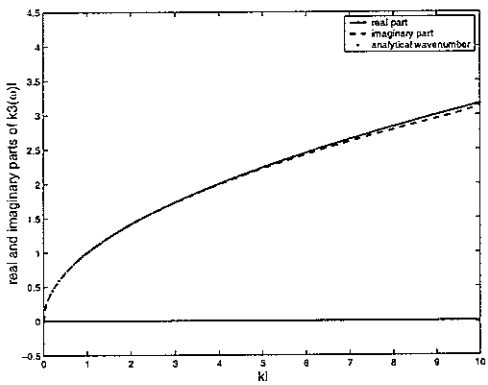

Figure 17: Dispersion relations for $k_3(\omega)$.

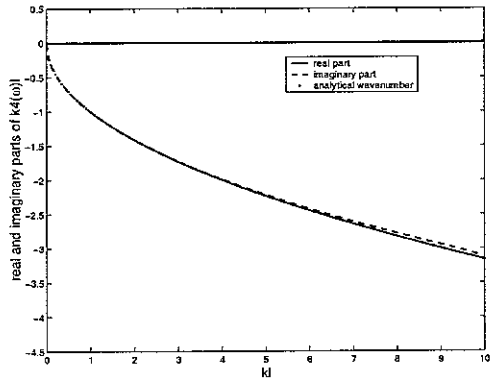

Figure 18: Dispersion relations for $k_4(\omega)$.

4.2.3 Frequency response

As a next step, we calculate the frequency response function (FRF) for the excitation by the force F at the position 2/3L. We do not give the complex expressions for the right and left eigenvectors. The relation between the forces and the displacements for a structure with N elements is, as given previously,

$$\begin{bmatrix} \mathbf{f}_L \\ \mathbf{f}_R \end{bmatrix} = \left(\begin{bmatrix} \mathbf{D}_{LL} & 0 \\ 0 & \mathbf{D}_{RR} \end{bmatrix} + \begin{bmatrix} \mathbf{D}_{LR} & 0 \\ 0 & \mathbf{D}_{RL} \end{bmatrix} \begin{bmatrix} \mathbf{P}_l^{N-1} & \mathbf{P}_r \\ \mathbf{P}_l & \mathbf{P}_r^{N-1} \end{bmatrix} \begin{bmatrix} \mathbf{P}_l^{N} & \mathbf{I} \\ \mathbf{I} & \mathbf{P}_r^{N} \end{bmatrix}^{-1} \right) \begin{bmatrix} \mathbf{q}_L \\ \mathbf{q}_R \end{bmatrix} \tag{4.20}$$

This relation is written for the parts of the beam respectively on the left and on the right of the force.

$$\begin{aligned} \begin{bmatrix} \mathbf{f}_L^1 \\ \mathbf{f}_R^1 \end{bmatrix} &= \mathbf{D}_1 \begin{bmatrix} \mathbf{q}_L^1 \\ \mathbf{q}_R^1 \end{bmatrix} \\ \begin{bmatrix} \mathbf{f}_L^2 \\ \mathbf{f}_R^2 \end{bmatrix} &= \mathbf{D}_2 \begin{bmatrix} \mathbf{q}_L^2 \\ \mathbf{q}_R^2 \end{bmatrix} \end{aligned} \tag{4.21}$$

with the following boundary conditions on the left and right sides and at the point where the force is applied.

$$\begin{cases} \mathbf{q}_L^1 = 0 \\ \mathbf{q}_R^1 = \mathbf{q}_L^2 \\ \mathbf{f}_R^1 + \mathbf{f}_L^2 + \begin{bmatrix} -F \\ 0 \end{bmatrix} = 0 \\ M_R^2 = 0 \\ v_R^2 = 0 \end{cases} \tag{4.22}$$

Assembling the matrices for the two parts of the beam and eliminating the fixed degrees of freedom, we get the global dynamic stiffness matrix. The displacements

and rotations can be obtained by the solution of the following system, where $\mathbf{D}_{tot}$ is the total dynamic stiffness matrix of the beam

$$\begin{bmatrix} F \\ 0 \\ 0 \end{bmatrix} = \mathbf{D}_{tot} \begin{bmatrix} v_L^2 \\ \theta_L^2 \\ \theta_R^2 \end{bmatrix} \tag{4.23}$$

The figures 19 to 22 give the analytical and numerical solutions for a beam with 3, 30, 3000 and 10000 elements. In this example, the cell is made of steel with $E = 2.10^{11} Pa$, $\rho = 7800\ kg/m^3$, $I = 8.33^{-14} m^4$, $L = 1m$, $S = 10^{-6} m^2$ and $F = 1N$. The displacement v_L^2 at the point where the force is applied is shown. A hysteretic damping with $\eta = 0.01$ is used. The results for 3 elements are clearly inaccurate except for very low frequencies, showing that the element size is too large in this case. The calculations for 30 and 3000 elements provide a very good comparison with the analytical solution. Thus the waveguide element approach is accurate for elements with very different scales and is essentially accurate if $kl < 2$. However, the case with 10000 elements shows the limits of the method when the element size becomes too small. The solution is not more accurate for small frequencies. This is not a real problem as the need for very small elements is for high frequencies in fact.

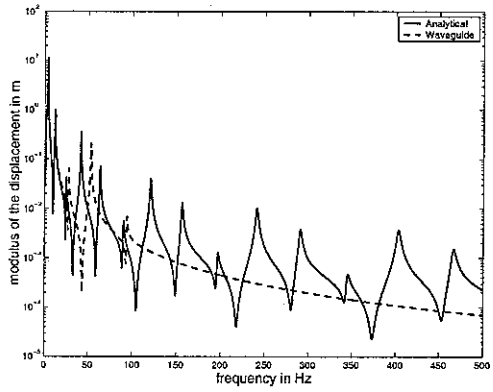

Figure 19: FRF for 3 elements.

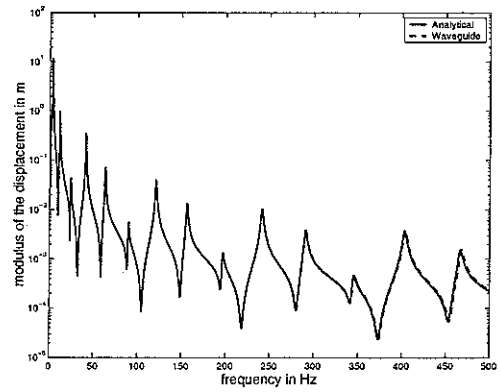

Figure 20: FRF for 30 elements.

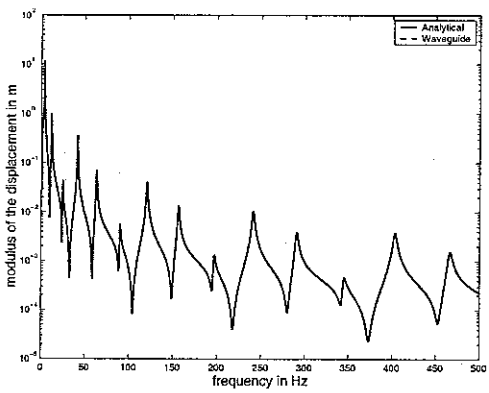

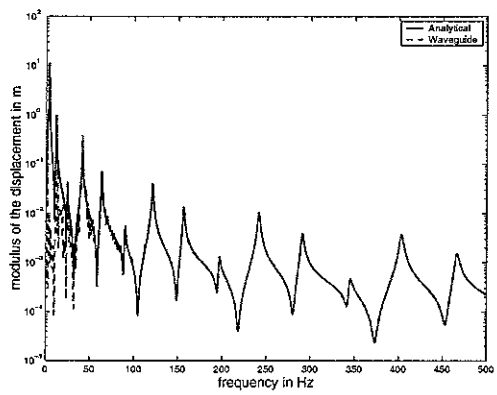

Figure 21: FRF for 3000 elements.

Figure 22: FRF for 10000 elements.

It must be noted that the calculation time is independent of the number of elements, which is a great advantage over classical finite element methods.

4.2.4 Change of scale of the mass and stiffness matrices

As the length of the cell l changes, so the elements of the mass and stiffness matrices change. This can be exploited to extend the frequency range of analysis without the need to remesh the structure. The mass matrix connects the displacements and rotations to the forces and moments. In a change of length of the beam cell, the displacements are proportional to the length and the rotation has no dimension. The density is conserved and the mass is proportional to the cross-sectional area times the length so is proportional to the length. As the acceleration is also proportional to the length, the force is proportional to the square length. Moments are proportional to the length to power three. This leads to the following table presenting the scale effect of a change of length of the beam on the physical quantities occurring in the mass matrix.

Physical quantity	Length effect	Exponent α
u	L	1
v	L	1
θ	1	0
F	L^2	2
M	L^3	3

Table 1: Scale effect for the mass matrix

For the stiffness matrix the displacements and rotations have the same behaviour with the length as for the mass matrix. The tangential and normal forces and the moments are changed according to the scale effect presented in table 2.

Physical quantity	Length effect	Exponent α
u	L	1
v	L	1
θ	1	0
F (tangential)	1	0
F (normal)	L^{-2}	-2
M	L^{-1}	-1

Table 2: Scale effect for the stiffness matrix

Consider now a matrix element connecting a force component F_i to a displacement component q_j with the relation $F_i = T_{ij} q_j$. If the exponent associated to F_i is α_i and the exponent of q_j is α_j, the coefficient T_{ij} will have the exponent $\alpha_i - \alpha_j$. This means that if the length of the element is changed from l_0 to l the coefficient is changed by $T_{ij} = \left(\frac{l}{l_0}\right)^{\alpha_i - \alpha_j} T_{ij}^0$. This relation allows new stiffness and

mass matrices for the length l to be calculated if we know these matrices for the length l_0.

As an example, figure 23 presents the FRF with the mass and stiffness matrices obtained from Ansys and scaled to have a beam with 30 elements. The parameters of the beams are the same as before. The original Ansys element had the length 0.02m and was rescaled. The figure proves the efficiency of the method.

In figure 24, the analytical solution is compared to an Ansys modal analysis with 30 and 300 elements. We used a modal damping with a constant factor equal to 0.005 for the Ansys calculation. Although this can explain a part of the difference between the numerical and analytical calculations, it is clear that the beam with 300 elements gives a solution closer to the analytical result. So a standard modal analysis needs a much larger number of elements to give the same accuracy as the waveguide approach.

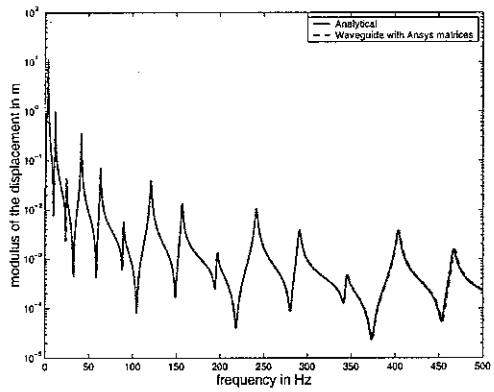

Figure 23: FRF for 30 elements with the Ansys matrices.

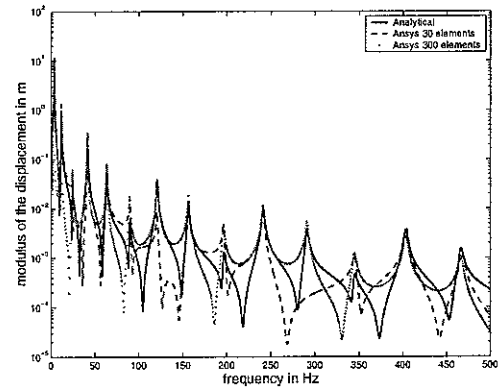

Figure 24: FRF by Ansys modal analysis with 30 and 300 elements.

4.3 Plate example

We consider now the example of the simply supported plate presented in figure 25 and under the action of a force F.

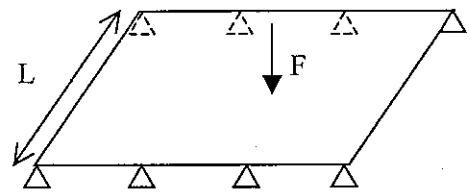

Figure 25: Simply supported plate

The equation describing the motion of the plate is

$$D\left(\frac{\partial^4 w}{\partial x^4}+2\frac{\partial^4 w}{\partial x^2\partial y^2}+\frac{\partial^4 w}{\partial y^4}\right)+\rho h\frac{\partial^2 w}{\partial t^2}=F \tag{4.24}$$

with $D=\frac{Eh^3}{12(1-\nu^2)}$ the bending stiffness, ρ the density, E the Young's modulus, ν the Poisson's ratio and h the thickness of the plate.

4.3.1 Dispersion relations

The analytical dispersion relations for the simply supported plate of width L is (see Fahy [20])

$$k_n^2=\omega\sqrt{\frac{\rho h}{D}-\left(\frac{n\pi}{L}\right)^2} \tag{4.25}$$

The numerical results are obtained from Ansys stiffness and mass matrices for the mesh presented in figure 26.

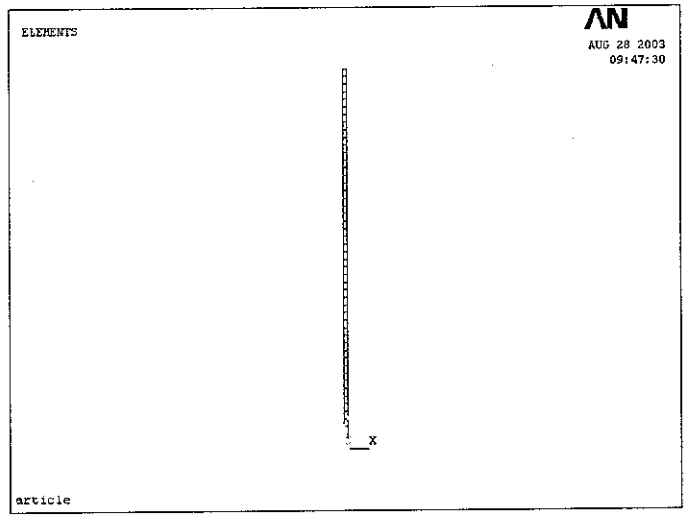

Figure 26: Ansys mesh with a layer of 50 shell elements.

Numerical dispersion relations can be obtained by plotting the curves $k_i(\omega)=\frac{1}{il}\log(\lambda_i(\omega))$ where l is the width of the layer equal here to $0.01m$. The results are given in figures 27 to 30. The example is a steel plate with a thickness $h=0.001m$ and a width $L=1m$. It can be observed that the propagating waves are correctly estimated as the real parts of the wavenumbers are close to the analytical solutions. The agreement on the number of propagating waves is also very good as can be seen in figure 30. A difference can be seen for the near-field waves mainly in figure 29. In fact, the numerical wavenumber number 5 was estimated by taking the fifth closest propagation constant to one. As the imaginary part of the wavenumber increases, mainly for low frequencies, the propagation constant becomes very small. The fifth analytical propagation constant becomes mixed with a large number of small

eigenvalues of the transfer matrix and it is difficult to separate the true propagation constants from the other eigenvalues.

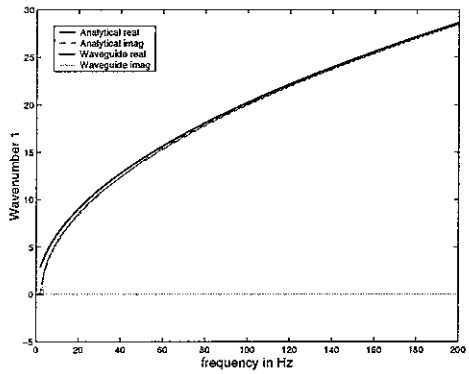

Figure 27: Dispersion relations for $k_1(\omega)$.

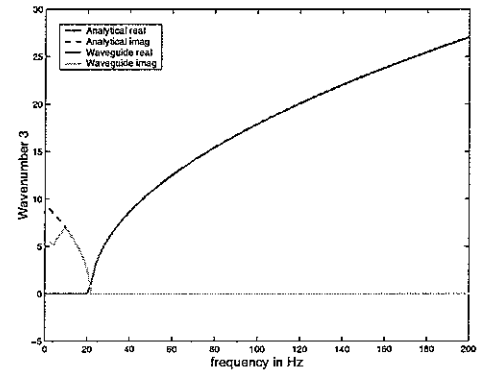

Figure 28: Dispersion relations for $k_3(\omega)$.

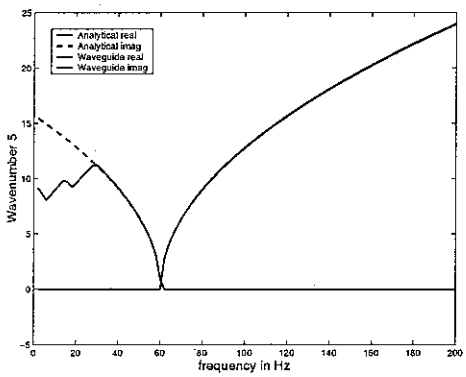

Figure 29: Dispersion relations for $k_5(\omega)$.

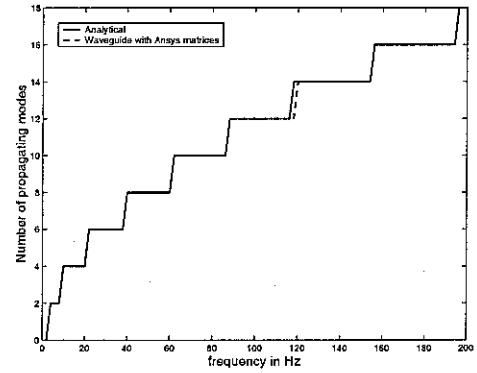

Figure 30: Number of propagating waves.

4.3.2 Frequency response

Next, we calculate the frequency response function (FRF) for the excitation by the force F at the middle of the plate. The relation between the forces and the displacements for a structure with N elements is, as given previously,

$$\begin{bmatrix} \mathbf{f}_L \\ \mathbf{f}_R \end{bmatrix} = \left(\begin{bmatrix} \mathbf{D}_{LL} & 0 \\ 0 & \mathbf{D}_{RR} \end{bmatrix} + \begin{bmatrix} \mathbf{D}_{LR} & 0 \\ 0 & \mathbf{D}_{RL} \end{bmatrix} \begin{bmatrix} \mathbf{P}_l^{N-1} & \mathbf{P}_r \\ \mathbf{P}_l & \mathbf{P}_r^{N-1} \end{bmatrix} \begin{bmatrix} \mathbf{P}_l^{N} & \mathbf{I} \\ \mathbf{I} & \mathbf{P}_r^{N} \end{bmatrix}^{-1} \right) \begin{bmatrix} \mathbf{q}_L \\ \mathbf{q}_R \end{bmatrix} \tag{4.26}$$

This relation is written for the parts of the plate respectively on the left and on the right of the force.

$$\begin{bmatrix} \mathbf{f}_L^1 \\ \mathbf{f}_R^1 \end{bmatrix} = \mathbf{D}_1 \begin{bmatrix} \mathbf{q}_L^1 \\ \mathbf{q}_R^1 \end{bmatrix}$$
$$\begin{bmatrix} \mathbf{f}_L^2 \\ \mathbf{f}_R^2 \end{bmatrix} = \mathbf{D}_2 \begin{bmatrix} \mathbf{q}_L^2 \\ \mathbf{q}_R^2 \end{bmatrix} \tag{4.27}$$

with the following boundary conditions on the left and right sides and at the point where the force is applied.

$$\begin{cases} \mathbf{q}_L^1 \text{ simply supported} \\ \mathbf{q}_R^1 = \mathbf{q}_L^2 \\ \mathbf{f}_R^1 + \mathbf{f}_L^2 + \mathbf{F} = 0 \\ \mathbf{q}_R^2 \text{ simply supported} \end{cases} \tag{4.28}$$

Assembling the matrices for the two parts of the plate and eliminating the fixed degrees of freedom, we get the global dynamic stiffness matrix. The process is the same as for the beam example. The displacements and rotations can be obtained by the solution of the following system, where $\mathbf{D}_{tot}$ is the total dynamic stiffness matrix of the beam

$$\mathbf{F}_{ext} = \mathbf{D}_{tot}\mathbf{q} \tag{4.29}$$

Figure 31 presents a comparison of the waveguide calculations and the analytical solution. The two results agree very well. Figure 32 compares the analytical solution with Ansys standard modal analysis for 10x10 and 100x100 elements. Clearly a mesh with 10x10 elements is not enough to get an accurate solution. The solution with 100x100 elements is accurate but at the price of a huge calculation in terms of time and memory reaching the limits of what can be done on a personal computer. Thus, the waveguide approach gives a much better solution with less computational resource.

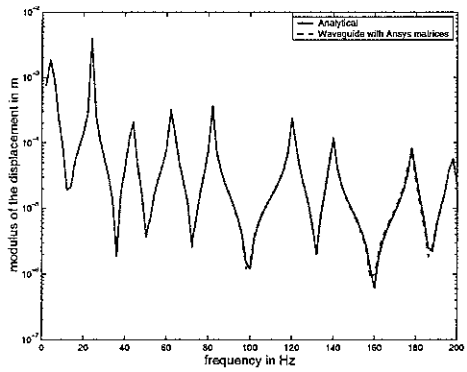

Figure 31: Comparison of analytical and waveguide results.

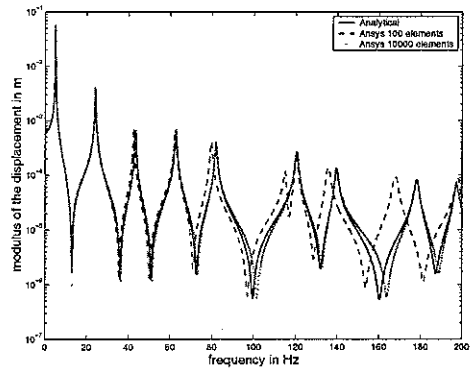

Figure 32: Comparison of analytical and Ansys modal analysis.

So, different examples were presented, some simple like the rod and the beam, and a larger one with the plate. The link with Ansys to get the stiffness and mass matrices allows dealing with more complex examples than these one. The dispersion relations were found and the accuracy of the propagating waves was found very good. For attenuating waves the wavenumbers need not be too small to be determined accurately. The force responses are also found in close agreement with the analytical solutions and are much better than those obtained by the standard modal analysis with Ansys.

5. Conclusions

In this report a numerical method for calculating the vibrations of periodic and waveguides structures was presented. The starting point of this approach is the dynamic stiffness matrix of a cell of the periodic structure, which is obtained from standard finite element software after meshing the cell and solving a simple dynamic problem to create the mass and stiffness matrices. For a periodic structure, we introduced the right and left propagation matrices, which are solutions of a recurrence equation. The global dynamic stiffness matrix of a structure with N cells is then obtained from these propagation matrices. One must notice that the calculation cost to get this global dynamic stiffness matrix does not depend on the number of cells N.

To analysis the structure in terms of waves, we introduced the transfer matrix linking the displacements and forces on both sides of a cell. Then, the propagation constants and the wave basis are respectively the eigenvalues and eigenvectors of the transfer matrix. This basis allows decomposing the state vector, made of the displacements and forces in a section, into wave amplitudes. Thus, the behaviour of a structure with N cells can be written in a simple way in terms of wave amplitudes and, after some transformations, the dynamic stiffness matrix of the global structure is obtained. This also gives formulas to calculate the propagation matrices.

The examples of a rod, a beam and a plate show that, at least for low frequencies, the numerical dispersion relations are very close to the analytical relations. This means that the accuracy of the present approach is good when the size of the cell is small compared to the wavelength. The point force response shows a similar agreement with the analytical calculations and seems better than pure finite element results obtained by the standard modal analysis for the same number of elements. If we compare to standard FE approaches, the cost of a calculation with the model developed in this paper is greatly reduced because we only have to mesh one cell instead of the whole structure. The other advantage is that standard FE packages can be used on the contrary of spectral FE, which need to develop new elements for each application. The model is also the same for any sort of damping, what could be used to introduce more accurate forms of damping than hysteretic or modal damping.

Some points could be improved. For instance, it would be interesting to use a reduced wave basis instead of using the whole set of eigenvectors and eigenvalues. However, the correct way of doing this is still an open question. One could study in more details the numerical instabilities found in section 4.2.3 when the size of the cell becomes very small to try to extend the domain of validity of the present approach. The use of the change of scale of the dynamic stiffness matrix presented in section 4.2.4 for a beam can also be extended to more general structures. Finally, we could try to extend this one-dimensional approach of wave propagation in one direction to two and three-dimensional propagations. This means that we could try to calculate the plate example of section 4.3 using only one finite element instead of the 50, which were used to model the strip. This last problem seems however more difficult than the other points.

References

1. D. WANG, C. ZHOU AND J. RONG, Free and forced vibration of repetitive structures, International Journal of Solids and Structures 40 (2003) 5477-5494.
2. L. BRILLOUIN, Wave propagation in periodic structures. New York: Dover, 1953.
3. D. J. MEAD, Wave propagation in continuous periodic structures: research contributions from Southampton, 1964-1995, Journal of Sound and Vibration 190 (1996) 495-524.
4. D. J. MEAD, A general theory of harmonic wave propagation in linear periodic systems with multiple coupling, Journal of Sound and Vibration 27 (1973) 235-260.
5. D. J. MEAD, Wave propagation and natural modes in periodic systems: I. Mono-coupled systems, Journal of Sound and Vibration 40 (1975) 1-18.
6. D. J. MEAD, Wave propagation and natural modes in periodic systems: II. Multi-coupled systems, with and without damping, Journal of Sound and Vibration 40 (1975) 19-39.
7. D. J. MEAD and N. S. BARDELL, Free vibration of a thin cylindrical shell with periodic circumferential stiffeners, Journal of Sound and Vibration 115 (1987) 499-520.
8. R. M. ORRIS and M. PETYT, A finite element study of harmonic wave propagation in periodic structures, Journal of Sound and Vibration 33 (1974) 223-236.
9. A. Y. A. ABDEL-RAHMAN, Matrix analysis of wave propagation in periodic systems, PhD thesis, University of Southampton, 1979.
10. D. J. THOMPSON, Wheel-rail noise generation, part III: Rail vibration, Journal of Sound and Vibration 161 (1993) 421-446.
11. A. H. VON FLOTOW, Disturbance propagation in structural networks, Journal of Sound and Vibration 106 (1986) 433-450.
12. L. S. BEALE and M. L. ACCORSI, Power flow in two- and three-dimensional frame structures, Journal of Sound and Vibration 185 (1995) 685-702.
13. S. FINNVEDEN, Finite element techniques for the evaluation of energy flow parameters, Proc. Novem, Lyon (keynote paper), 2000.
14. C. M. NILSSON, Waveguide finite elements for thin-walled structures, Licentiate thesis, KTH, Stockholm, 2002.
15. P. J. SHORTER, Wave propagation and damping in linear viscoelastic laminates, Journal of the Acoustical Society of America. Submitted for publication.
16. L. GRY, Dynamic modelling of railway track based on wave propagation, Journal of Sound and Vibration 195 (1996) 477-505.
17. L. GRY and C. GONTIER, Dynamic modelling of railway track: a periodic model on a generalized beam formulation, Journal of Sound and Vibration 199 (1997) 531-558.
18. W. X. ZHONG and F. W. WILLIAMS, On the direct solution of wave propagation for repetitive structures, Journal of Sound and Vibration 181 (1995) 485-501.
19. M. PETYT, Introduction to finite element vibration analysis, Cambridge University Press, New York, USA, 1990
20. F. FAHY, Sound and structural vibration, Academic Press, London, 1987.